ADVANCED HEALTHCARE MATERIALS
www.advhealthmat.de

Interactions of Neurons with Physical Environments

*Michal Marcus, Koby Baranes, Matthew Park, Insung S. Choi, Kyungtae Kang, and Orit Shefi**

Nerve growth strongly relies on multiple chemical and physical signals throughout development and regeneration. Currently, a cure for injured neuronal tissue is an unmet need. Recent advances in fabrication technologies and materials led to the development of synthetic interfaces for neurons. Such engineered platforms that come in 2D and 3D forms can mimic the native extracellular environment and create a deeper understanding of neuronal growth mechanisms, and ultimately advance the development of potential therapies for neuronal regeneration. This progress report aims to present a comprehensive discussion of this field, focusing on physical feature design and fabrication with additional information about considerations of chemical modifications. We review studies of platforms generated with a range of topographies, from micro-scale features down to topographical elements at the nanoscale that demonstrate effective interactions with neuronal cells. Fabrication methods are discussed as well as their biological outcomes. This report highlights the interplay between neuronal systems and the important roles played by topography on neuronal differentiation, outgrowth, and development. The influence of substrate structures on different neuronal cells and parameters including cell fate, outgrowth, intracellular remodeling, gene expression and activity is discussed. Matching these effects to specific needs may lead to the emergence of clinical solutions for patients suffering from neuronal injuries or brain-machine interface (BMI) applications.

1. Introduction

The limited repair capacity of the central and peripheral nervous systems leads to a strong interest in developing new strategies for promoting nerve regeneration. Extensive research efforts are currently ongoing globally, developing interfaces with neuronal tissues for discerning fundamental mechanisms of growth and for biomedical applications.[1–6] Neuronal damage, caused either by neurodegenerative diseases or by physical injury, is manifested by various cellular mechanisms that have yet to be fully discovered. Currently, clinicians caring for patients with such injuries, have very little in their arsenal to meet this pressing medical need. Neuronal damage is multifaceted: it affects function, morphology, activity and circuity of neurons. As the complexity of the nervous tissue makes it difficult to investigate neuronal functions in vivo, researchers have attempted to mimic the neurons' extracellular environment using carefully engineered platforms. These engineered substrates that come in 2D and 3D forms—to isolate specific regenerative mechanisms and to mimic real systems—can eventually lead to the development of neural devices and new therapies for effective neuronal regeneration.

During the development of the nervous system, neurons differentiate from stem cell precursors to mature, functional neurons. During this period, neuronal processes outgrow and form numerous connections with neighboring cells in a trial-and-error-based progression, ultimately developing into complex neuronal networks.[7–9] These neuronal processes elongate and bifurcate in response to orchestrated signals from the extracellular environment that affect the growth pattern and organization of the developing nervous system. A key mechanism in neuronal development is the actions of the growth cone at the tip of a growing process to measure such environmental cues and use them to grow accordingly.[10–13] Growth cones are directed to their targets by responding to repulsive or attractive chemical cues.[13,14] Soluble and matrix-bound factors, such as neurotrophins[15–17] and axon guidance molecules,[18–21] determine the neuronal behaviors including lineage, morphogenesis and neurite growth rate.[7,22] In addition to the biochemical aspect of the extracellular environment, neuronal growth is also affected by the physical features of the environment, through interactions with contact guidance. Studies have shown that contact guidance, which is dependent on the physical shape of the substratum, induces alignment (i.e. directional growth) of cells in a developing brain.[23] The extracellular matrix (ECM) exhibits micron and sub-micron scale structures that are sensed by filopodia of a growth cone during neurite outgrowth. Neurite filopodia probe the surrounding extracellular microenvironment

M. Marcus, Dr. K. Baranes, Prof. O. Shefi
Faculty of Engineering and Bar-Ilan Institute for Nanotechnology and Advanced Materials
Bar-Ilan University
Ramat-Gan 5290002, Israel
E-mail: orit.shefi@biu.ac.il
M. Park, Prof. I. S. Choi
Center for Cell-Encapsulation Research
Department of Chemistry
KAIST
Daejeon 34141, Korea
Prof. K. Kang
Department of Applied Chemistry
Kyung Hee University
Yongin, Gyeonggi 17104, Korea

DOI: 10.1002/adhm.201700267

during neuronal growth cone pathfinding, and these cytoskeletal structures, rich in microtubules and actin filaments, yield traction forces that push or pull the neurite forward or backward, respectively.[24–26] Several receptors have been suggested to be involved in these signaling pathways which are triggered during growth cone pathfinding, e.g. the cell adhesion molecule CD44,[27] DCC[28] and distinct integrins.[29,30]

Understanding neurite contact guidance is of critical importance for the design of synthetic nerve scaffolds and for the generation of modern neuronal-based devices. When natural reconstruction is not possible, a scaffold of biomaterial can act as a bridge, providing structural support for neuronal cell growth and guiding nerve regeneration during the repair of nerve injuries.[23,31–34] In addition, interactions between neurons and physical elements can be utilized for the construction of a stable, high-resolution electronic interface to neurons, which will be required for future brain-machine interfaces (BMIs).[35–40]

Neuronal morphology and function are known to be closely linked, reciprocally affecting one another. Thus, determining the effect of an engineered surface on cellular growth and morphology gives an indication of the efficacy of the combined material and geometry for promoting a specific and desired response.[41] Such understanding is crucial for the development of new therapeutic intervention strategies for nerve repair, and can also shed light on the underlying mechanisms of neuronal regeneration and circuity.

Recent advances in micro- and nanofabrication techniques have enabled the construction of substrates that recapitulate the structure and scale of native topography.[42–45] Similar to native neuron-topography interactions, neurons were shown to respond to synthetic topographic substrates, e.g. electrospun fibers,[46–48] isotropic features and anisotropic features.[11,12,35,49–51] These interactions depended on many factors, including cell type, feature size and geometry.[42,52] Various other physical properties of the substrate, such as stiffness and roughness, played significant roles as well,[53] and could be additionally modified chemically for further levels of interaction.[26]

In this review, we survey the interactions between neurons and various physical topographic environments. We discuss commonly used topographical structures for neuronal studies, their use-cases, and the morphological as well as behavioral characterizations conducted on these surfaces including neural directionality, morphology and adhesion. These interactions serve as basic principles for the design of therapeutic applications. To have a better understanding of neuronal interactions with native and synthetic extracellular environments, we also review studies that examined the immediate effects of topographies on growth patterns as well as on the molecular responses, differentiation, and activity. Finally, we discuss how, by adapting topographical features to 3D environments, these effects can be utilized for applications in tissue engineering and regenerative medicine, as illustrated in **Figure 1**.

Michal Marcus is a Ph.D. candidate in the Faculty of Engineering, Department of Bioengineering at Bar Ilan University in Israel, where she also obtained her M.Sc. degree in Bioengineering in 2013. Before moving to Engineering, she has completed a B.Sc. in Biotechnology at Bar Ilan University. Her research focuses on magnetic nanoparticles for magnetic manipulations on neuronal cells for regeneration and therapeutic applications.

Koby Baranes completed M.Sc. studies in Neurobiology at Tel-Aviv University, Israel in 2009 and received his Ph.D. in Bioengineering in 2016 from the Faculty of Engineering at Bar-Ilan University, Israel. His thesis focused on the interactions of neurons with 2D and 3D platforms as a method for designing neural networks and for regeneration. Currently he is a research associate at the Department of Clinical Neurosciences at the University of Cambridge, United Kingdom. His research interests are in the field of neuronal regeneration and therapeutic approaches.

Orit Shefi is an Associated Professor in the Faculty of Engineering and a member of the Institute of Nanotechnologies and Advanced Materials at Bar Ilan University, Israel. She is the head of Neuroengineering and Regeneration Laboratory. She joined Bar Ilan University after graduating in Physics at Tel-Aviv University, Israel in 2005, and performing a postdoctoral work in the Division of Life Sciences at the University of California, San Diego, USA.

2. Topographical Features for Neuronal Platforms

Various types of substrates serve as platforms for neuronal culture, including 2D petri-dishes in vitro, planar sheets and needles, 3D scaffolds, guiding channels in vivo, etc. The characteristics of the substrate affect neuronal response and interaction with the substrate. Beside topography, substrate material has also been found to greatly affect neuronal growth.[54–58] Nevertheless, this review focuses on topographical

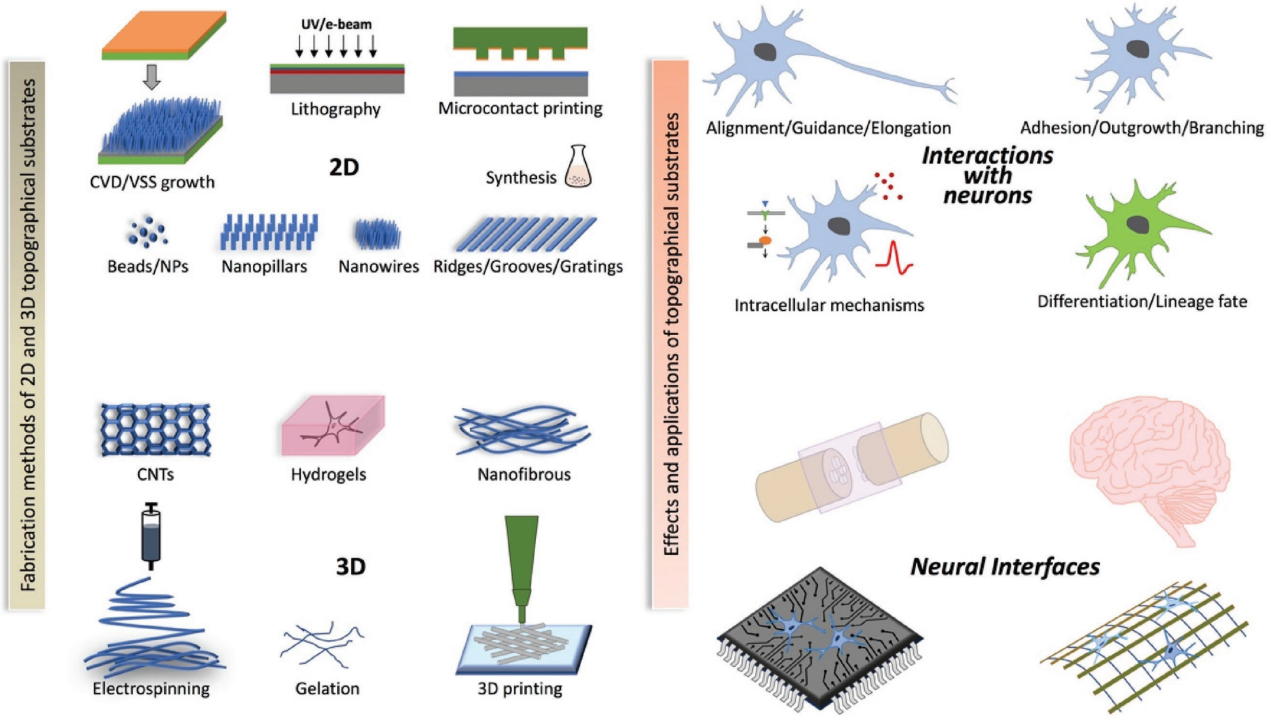

Figure 1. (Left) An overview of the major topographical elements that are used and reviewed for modifying physical environment of neurons. (Right) Schematic illustration of typical effects of topographical substrates on neurons and the potential use of topography for neural interfaces for in vitro and in vivo setups.

effects and does not cover the aspect of material type. We focus on those which are commonly used with relevance to potential biomedical applications. In this section, we describe topographical features which include anisotropic topography ("continuous features"), such as grooves and ridges, and isotropic topography ("interrupted features"), such as pillars and nanowires.

2.1. Anisotropic Topography

One of the first topographical structures featured in neuronal studies was grooves. Parallel grooves have been used extensively to characterize the in vitro behavior of several other cell types, as well as neuronal cultures to some extent.[59–62] The initial goal was to create a platform that promoted the organization of aligned radial glia and subventricular cells found in a developing brain, which could act as tracts that direct neuronal growth and migration.[63] As a result, neuronal contact guidance, which is a critical neurodevelopmental phenomenon that occurs in vivo,[64,65] could now be easily observed and characterized in an in vitro setting.[51,63,66–70]

The advance in fabrication techniques, such as lithography, provided a wider availability of complex topographical structures for neuronal studies, as demonstrated in **Figure 2**A and in **Table 1**, which summarize the studies discussed in this review. As one of the primary methods for fabricating topographical substrates, lithography offered a means of producing grooved patterns at both micrometer and nanometer scales. While the types of lithography used can vary (e.g. photolithography, electron-beam lithography, soft lithography, etc.), the desired substrates could be produced consistently and uniformly. Earlier studies, which have been limited to the use of micrometric channels or grooves, could now become more sophisticated and be conducted on grooves with nanometric ridges with variable widths, gaps, and depths.[71,72] Ultimately, finer control over topographical features increased the level of control over neuronal behaviors and morphologies as well. For instance, nanogratings (and similar features) were used not only to observe filamentous filopodial protrusions (≈200 nm) but were also employed to control the alignment and orientation of individual focal adhesions (FAs).[50,63,70,73,74]

As a 3D platform, electrospun fibers from polymer solutions were developed with the ability to align the fibers in a parallel orientation.[48,75–77] The produced nanofibers create a mesh (scaffold) which can mimic the native neuronal ECM and provide topographical, biochemical and mechanical cues for proper organization and tissue formation.[78,79] In addition to the wide variety of materials that can be used, such as poly(L-lactic acid) (PLLA)/ poly(lactic-co-glycolic acid) (PLGA), polycaprolactone (PCL), poly(vinyl alcohol) (PVA), or collagen, fiber diameter and orientation can be modified, as well, to some extent. In addition, the fibers can be further manipulated by adding, for example, nanoparticles atop the fibers (Figure 2B).[46] Additional manipulations can vary, from the use of conductive materials (such as graphene),[80,81] to the incorporation of siRNA to functionalize the fibers.[82] With their low cost, high production rate and biocompatibility, these fibers are an optimal basis for many applications that require axon guidance or even elongation,

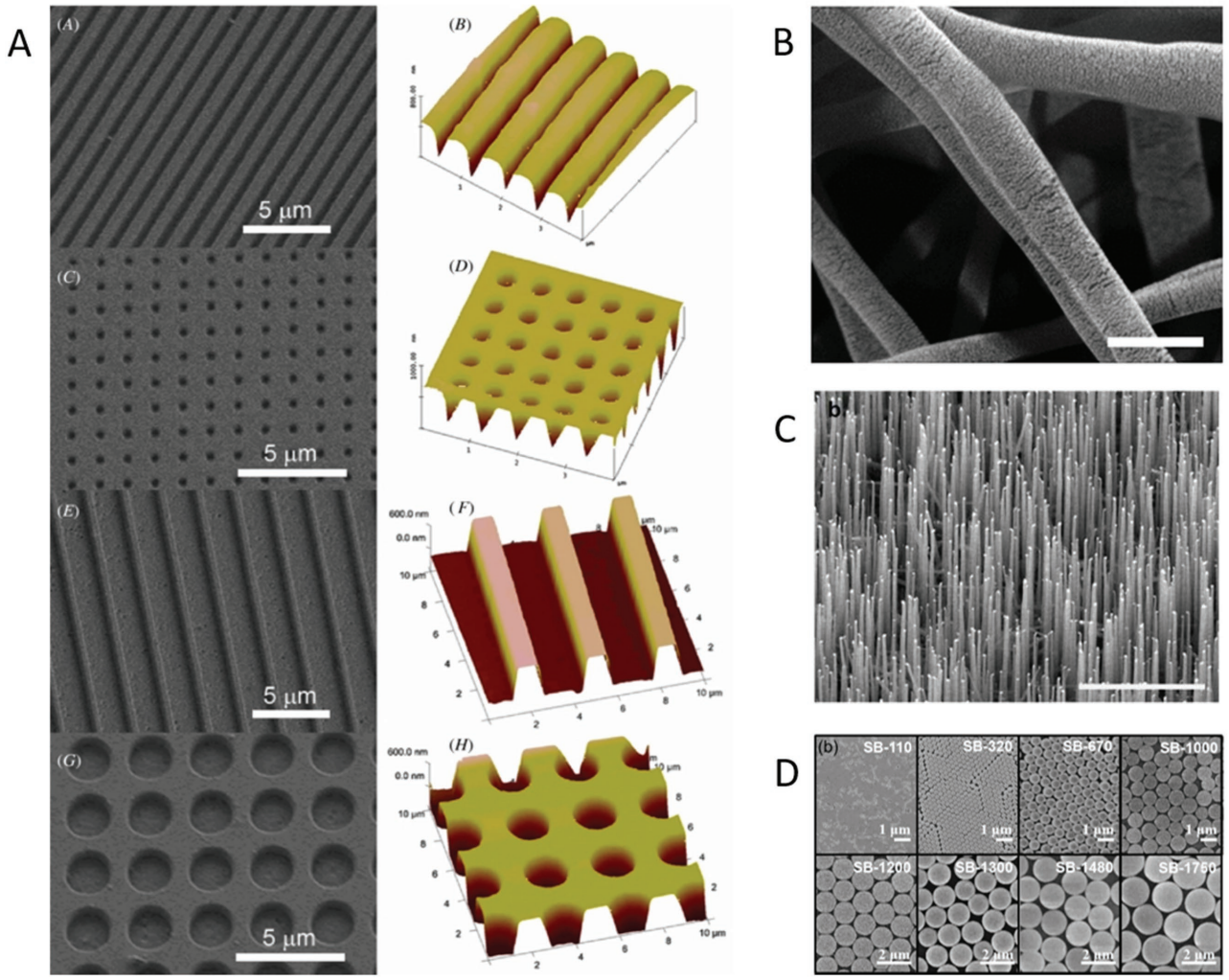

Figure 2. A) Quartz surfaces patterned with arrays of structures to form topographies of grooves (lines) (A, B, E and F) and holes (C, D, G and H). Reproduced with permission.[51] Copyright 2010, IOP Science. C) A Scanning electron microscopy (SEM) image of Au-catalyzed *vg*-SiNWs. Scale bars 5 μm. Reproduced with permission.[85] Copyright 2016, American Chemical Society. B) An ESEM image of AuNPs on the surface of electrospun fibers. Scale bar 500 nm. Reproduced with permission.[46] Copyright 2016, American Chemical Society. D) SEM images of 110–1750 nm silica beads (SB) monolayers. Reproduced with permission.[89]

including, among others, spinal cord repair, drug delivery systems and implants.[8,75,83]

2.2. Isotropic Topography

Unlike grooves and fibers, nanowires and pillar structures act as "interrupted" rather than "continuous" topographical features. These structures can limit cell adhesion sites to highly concentrated contact points, which have been shown to elicit a variety of different neuronal behaviors, including developmental acceleration, as well as alternative pathways to neuritogenesis.[39,84,85] Additionally, nanowire and pillar structures can be ordered in various organizations, from stochastic arrangements, to uniform arrays, and even anisotropic rows (Figure 2C).[49,86,87] This allows researchers to not only modify the extent of contact between the cell surface and substrate, but also to influence neurite directionality, in addition to their rate of development.

Like nanowire/pillar substrates, several other types of topographical structures have been used to present neurons with an "interrupted" physical environment. The smooth, flat, standard substrates of neuronal cultures are a poor representation of the structurally complex fibrous composition of the ECM in vivo. As a more suitable alternative, different topographical structures have been used to replicate the discontinuous nature of the natural environment of a neuron in a quantifiable manner. For instance, the concave structure of anodized aluminum oxide has been shown to elongate neurite length and to accelerate neuronal development. This acceleration depended on the pitch of the topographical features and was not simply a binary mechanism.[88] Further study utilizing silica bead arrays revealed that in topographically-induced developmental acceleration, there is an upper and a lower threshold that correlates

Table 1. Summary of topographies and their effects on neuronal cells.

Feature type	Material	Method	Width/Diameter	Depth/Height	Neuronal cell type	Effect(s)	Ref.
Beads	Sepharose 4B	N/A[a)]	60–80 µm	N/A	Rat cerebellum; Neonatal cerebellar neurons	Synaptic elements	[129]
Beads	Silica (coated)	Commercial	500 nm, 5–7 µm	N/A	Hippocampal neurons	Synaptic elements	[130–132]
Beads	Silica	TEOS[b)] hydrolysis	100–700 nm	N/A	E18 rat Hippocampal neurons	Outgrowth; Elongation	[88]
Channels	PDMS	Lithography	1, 2 µm	400, 800 nm	Hippocampal neurons	Polarity; Elongation; Directionality	[68,99]
CNT/OTS[c)] patterns	Carbon; OTS	Commercial CNTs; Photolithography	10 µm	N/A	E18 rat Hippocampal neurons	Outgrowth; Guidance; Elongation; Network formation	[110]
CNTs	Carbon	N/A	N/A	N/A	Mouse organotypic spinal cord explants	Network formation	[175]
CNTs	Carbon	Commercial	N/A	N/A	Hippocampal neurons	Electrical activity; Synaptic elements	[174]
Dots	Tantalum oxide	AAO[d)] processing	50, 100, 200 nm	N/A	C6 glioma astrocytoma	Focal adhesion; Gap junctions	[128]
Fibers (Aligned)	PLLA	Electrospinning	150–500 nm; 800–3000 nm	N/A	C17.2 neural stem cells	Guidance; Directionality; Outgrowth; Differentiation	[47]
Fibers (Aligned)	PLLA	Electrospinning	500 nm	5–10 mm	DRG	Outgrowth; Guidance	[75]
Fibers (Aligned)	PAN-MA[e)]	Electrospinning	400–600 nm	N/A	DRG neurons	Guidance; Directionality; Outgrowth; Electrical activity	[31]
Fibers (Aligned)	PCL/gelatin	Electrospinning	160–200 nm; 230–470 nm	N/A	Rat Schwann cells	Guidance; Directionality; Axon support	[114]
Fibers (Aligned)	PCL	Electrospinning	N/A	N/A	DRG	Guidance; Directionality; Adhesion; Outgrowth; Elongation	[26,115]
Fibers (Aligned)	PCL	Electrospinning	250 nm	N/A	CE3 and RW4 mouse embryonic stem cells	Differentiation; Neural lineage; Elongation	[83]
Fibers (Aligned)	PLLA	Electrospinning	600–800 nm	N/A	Primary motor neurons	Neuritogenesis; Guidance; Directionality	[8]
Fibers (Aligned)	PCL	Electrospinning	1 µm; 250 nm	N/A	Neural precursors	Differentiation; Neural lineage	[137]
Fibers (Aligned)	TSF[f)]	Electrospinning	400, 800 nm	N/A	Human embryonic stem cells	Differentiation	[145]
Fibers (Aligned)	Collagen	Gelation	N/A	N/A	*Hirudo medicinalis* Leech neurons; PC12	Guidance; Directionality; Branching	[112,113]
Fibers (Random)	PES[g)]	Electrospinning	283, 749, 1452 nm	N/A	Neural stem cells	Differentiation; Neural lineage	[144]
Fibers (Random)	PCL	Electrospinning	260, 480, 930 nm	N/A	Adult neural stem cells	Differentiation	[146]
Fibers (Random)	PCL/gelatin	Electrospinning	260 nm	N/A	*Hirudo medicinalis* Leech neurons; PC12	Branching; Outgrowth; Differentiation; Elongation	[46]
Fibers (Modified)	PCL	Electrospinning; siRNA	542–548 nm	N/A	Mouse neural progenitor cells	Differentiation; Neural lineage	[82]
Gratings	PDMS	Lithography	350 nm; 1, 10 µm	350 nm	Human mesenchymal stem cells	Differentiation; Width effect; Neural lineage	[141]
Gratings	TCPS[h)]	NIL[i)]	500, 750 nm	200 nm	PC12 cells	Guidance; Directionality; Width effect	[103]
Gratings	COC[j)]	NIL	500–2000 nm	350, 500 nm	PC12 cells	Directionality; Width effect; Focal adhesion; Differentiation; Polarity; Guidance	[50,71]
Gratings	PDMS	Laser inference lithography	350 nm; 2, 5 µm	300 nm	Human induced pluripotent stem cells	Differentiation; Width effect; Neural lineage	[72]
Gratings	PDMS	Lithography	2 µm	0.35, 0.8, 2, 4 µm	Neural progenitor cells	Directionality; Differentiation; Neural lineage; Computational model	[98]
Gratings	COC	e-beam lithography	500 nm, 1 µm	350 nm	Hippocampal neurons	Cytoskeleton reorganization; Focal adhesion; Network formation; Branching	[122]

Table 1. Continued.

Feature type	Material	Method	Width/Diameter	Depth/Height	Neuronal cell type	Effect(s)	Ref.
Gratings/Pillars	PDMS	NIL	1–2 μm; 250 nm	80–250 nm; 2 μm	Murine neural progenitor cells; Human embryonic stem cells	Differentiation; Neural lineage	[135,136]
Grooves	Quartz (SiO_2)	Lithography	1–8 μm	0.05–0.8 μm	CNS neuroblasts	Guidance; Directionality	[69]
Grooves	PDLA[k]; PLGA	Indirect transfer techniques	10 μm	1–4 μm	DRG neurons	Outgrowth; Directionality; Branching	[93]
Grooves	PSPI[l]	Photolithography	20–60 μm	11 μm	PC12 cells	Guidance; Directionality; Width effect; Outgrowth; Branching	[107]
Grooves	PMMA	e-beam lithography	100–400 nm	300 nm	Sympathetic and sensory ganglia neurons	Guidance; Directionality; Width effect	[35]
Grooves	PDMS	Micro-contact printing; Micro-molding	10 μm	1 μm	Hippocampal neurons	Guidance; Directionality	[97]
Grooves	PLGA	Laser ablation	5, 10 μm	2–3 μm	PC12 cells	Guidance; Directionality; Width effect; Branching	[23]
Grooves	PDMS	Photolithography	5, 10, 20, 60 μm	25 μm	Human neural progenitor cells	Differentiation; Polarity; Outgrowth	[140]
Grooves; Ridges	Quartz (SiO_2)	e-beam lithography	1–4 μm	14–1100 nm	Hippocampal neurons; Embryonic *Xenopus* spinal cord neurons	Guidance; Directionality; Cytoskeleton reorganization	[63,74]
Grooves; Ridges	Quartz (SiO_2)	e-beam lithography	300 nm; 2 μm	400, 500 nm	Hippocampal neurons	Guidance; Directionality; Cell adhesion; Polarity	[51]
Nanoparticles	Ag	Deposition	110 nm	N/A	SH-SY5Y cells	Outgrowth	[118]
Nanoparticles	Iron oxide	Synthesis	100 nm	N/A	PC12 cells	Differentiation	[147]
Nanowires	Gallium phosphide	VSS[m] growth mode	50–70 nm	1.5–3 μm	DRG neurons; SCG[n]	Guidance; Focal adhesion; Outgrowth	[86,87]
Nanowires	Si	CVD[o]	70 nm	7–10 μm	E18 rat Hippocampal neurons	Neuritogenesis; Elongation; Electrical activity	[85]
Pillars	Si, Quartz (SiO_2)	Ion-beam and e-beam lithography	150 nm	1 μm	Embryonic cortical neurons	Electrical activity; Focal adhesion	[39]
Pillars	Quartz (SiO_2)	Lithography	1–5.6 μm	3 μm	Hippocampal neurons	Polarity; Focal adhesion; Elongation	[84]
Pillars	Quartz (SiO_2)	Photolithography	1 μm	5 μm	Hippocampal neurons	Guidance; Directionality	[49]
Pillars; Pores	Au	Electrodeposition	200 nm	2 μm	PC12 cells	Outgrowth; Elongation; Differentiation	[119]
Ridges	Quartz (SiO_2)	X-ray lithography	70–1900 nm	600 nm	PC12 cells	Differentiation; Outgrowth	[148]
Ridges	SiO_2	Photolithography	N/A	4 μm	Mouse N2a neuroblastoma	Guidance; Directionality	[96]
Ridges	PUA[p]	UV-assisted capillary force Lithography	350 nm	350 nm	Cortical neurons; N1E-115 neuroblastoma	Guidance; Directionality; Width effect	[102]
Ridges	V_2O_5	Photolithography	3 μm	10–150 nm	*Hirudo medicinalis* Leech neurons	Guidance; Directionality; Adhesion; Branching; Outgrowth; Network formation; Elongation	[12]
Ridges	Si	Photolithography	2, 10 μm	4 μm	Adult neural stem cells	Differentiation; Neural lineage	[134]
Roughness	Au	Wet chemistry (SGDR[q])	N/A	36–100 nm	SH-SY5Y cells	Cell adhesion; Polarity; Electrical activity	[73]
Spines	Au	Photolithography	0.85–1.84 μm	1.5 μm	*Aplysia californica* neurons	Electrical activity	[168,169]

[a]Not available; [b]Tetraethyl orthosilicate; [c]Octadecyltrichlorosilane; [d]Anodic aluminum oxide; [e]Poly(acrylonitrile-co-methylacrylate); [f]Tussah silk fibroin; [g]Poly(ethersulfone); [h]Tissue culture polystyrene; [i]Nanoimprint lithography; [j]Cyclic olefin copolymer; [k]Poly-D,L-lactic acid; [l]Photosensitive polyimide; [m]Vapor-solid-solid; [n]Superior cervical ganglia; [o]Chemical vapor deposition; [p]Polyurethane acrylate; [q]Spontaneous galvanic displacement reactions.

to sizes detectable by axons and filopodia, respectively (Figure 2D).[88,89]

3. Topography Effects on Neuron Morphology

Interactions between neurons and topographical features show diverse trends due to combinatorial effects exerted by topography and by the substrates' chemical properties.[90–94] Moreover, neuron-topography interactions vary across neuron origin, feature dimension and feature geometry. However, there are general topography effects that are commonly found throughout neuronal growth and may serve as basic principles in the design of a substrate for engineered neuron structures. Here, we discuss several fundamental aspects of neuronal cells and neuronal networks which are affected by topographical structures, both on planar surfaces and on 3D constructs.

3.1. Neuronal Guidance and Directionality

The most profound and well-studied effect of topography on neurons is the impact on cell directionality. The primary goal of neural tissue engineering is to guide neurite extension in a desired direction, thus, the ability to direct the alignment of the neuronal soma or of the extending neurites is highly valued.[41,95] Numerous studies have demonstrated that neurons respond to anisotropic patterns by aligning and elongating in the direction of the patterned structure. Neurites extending from the cell soma follow the axis of the topographical pattern, as does the soma itself, which 'spreads out' exhibiting an elongated morphology. Anisotropic topography, rather than isotropic topography, exerts a more pronounced effect on neuron directionality and orientation. Linear structures such as the grooves and ridges affect the direction of axonal growth when these structures are of micron sizes, a scale similar to that of axons. For example, neuron-like PC12 cells were cultured on micro-patterned films of PLGA with a depth of 2–3 μm and 5 and 10 μm wide grooves, guiding the direction of neurite outgrowth parallel to the microgrooves.[23] Similarly, mouse N2a neuroblastoma cells, cultured on patterned substrates of SiO_2 linear ridges with 4 μm height, extended their neurites following the linear microtrack.[96] In another study, rat hippocampal neurons were cultured on PDMS grid patterns of 1 μm height.[97] Neurite outgrowth was well-confined by the 10 μm width patterns which resulted in ordered neuronal networks. Furthermore, neurite alignment was observed to increase with grating depth, strongly supporting the hypothesis that extending neurites sense the depth of the underlying topography.[93,98] Although neuron directionality was found to be mostly achieved by linear anisotropic topography, vertical structures were reported to affect neuronal growth as well. For example, controlled neurite directionality was successfully demonstrated in primary hippocampal neurons by using interrupted vertical pillar array substrates with interpillar distances of 3 μm (**Figure 3**A).[49] While the majority of neurons aligned along the substrate's anisotropic pattern, namely exhibiting *parallel contact guidance*, an additional form of guidance was reported for specific neuron types—*perpendicular contact guidance*—in which neurites extend across the substrates, perpendicular to the axis of the patterned lines.[63,74] Perpendicular contact guidance was demonstrated by primary hippocampal neurons[51,74,99] and central nervous system (CNS) neuroblasts,[69] in a manner dependent on surface feature sizes. Hippocampal neurites grew parallel to deep, wide grooves but perpendicular to shallow, narrow ones. Interestingly, the frequency of perpendicular alignment of hippocampal neurites depended on the age of the embryos from which neurons are isolated, suggesting that contact guidance is regulated during development. Perpendicular orientation of CNS neuroblasts was frequently observed when the micro-structured grooves had depths between 0.3 μm and 0.8 μm and a width of 1 μm.

3.1.1. Feature Dimensions Role

Since cell adhesion sites, namely focal adhesions, are in the range of 5–200 nm,[100] it was suggested that cell–substrate

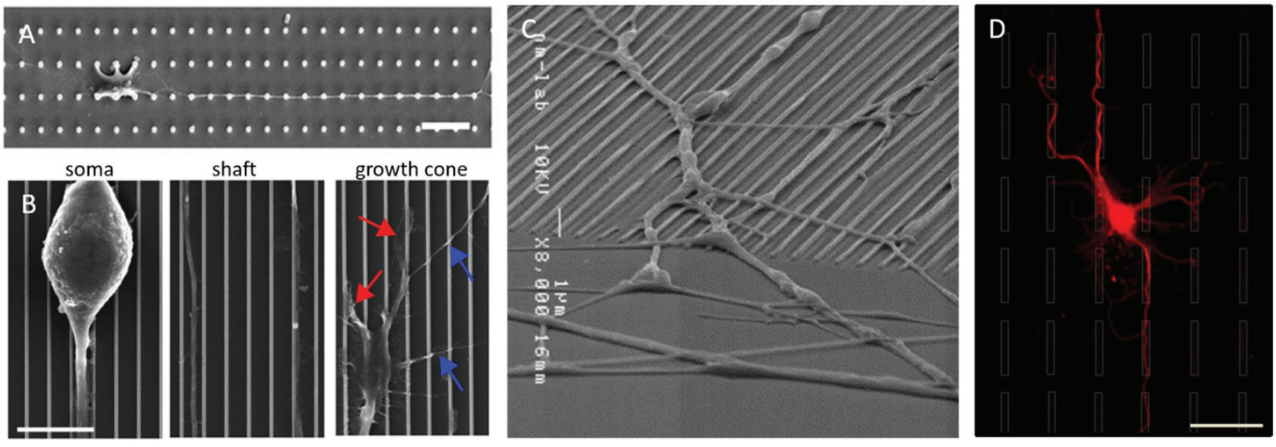

Figure 3. A) A SEM image of a primary hippocampal neuron on an anisotropic pillar array. Scale bar 10 μm. Reproduced with permission.[49] B) SEM images of N1E-115 cells plated on line substrates. Red arrows, aligned filopodia; Blue arrows, non-aligned filopodia. Scale bar 10 μm. Reproduced with permission.[102] Copyright 2010, PLOS. C) A SEM image showing axons alignment to 100 nm high and 100 nm wide ridges. Reproduced with permission.[35] Copyright 2009, Elsevier. D) A confocal microscopy image of an immunostained neuron (against α-tubulin) growing onto ridges of 50 nm height. Ridges locations are marked as white frames in the image. Scale bar 50 μm. Reproduced with permission.[11]

interactions are typically governed by complex mechanisms operating at the nanoscale and are strongly influenced by nanoscale features rather than microscale structures.[73,101] Indeed, recent studies have demonstrated neuron sensitivity to nanometer-sized topographic cues. Nano-topography, in this review, refers to topographical structures with sizes up to 500 nm. We have shown that neuronal processes of micron size can be directed by topographic cues that are an order of magnitude smaller, as low as 10 nm.[11] In a different study, embryonic Xenopus spinal cord neurons, grown on quartz etched with a series of parallel grooves, exhibited neurite growth parallel to grooves as shallow as 14 nm.[63] Neurites grew faster in the favored direction of orientation and turned through large angles to align on grooves. Higher nano-ridges of parallel lines (350 nm wide, 350 nm high) directed the neurites of primary cortical neurons and N1E-115 neuroblastoma (Figure 3B).[102] The same trend was observed on patterns of parallel grooves with depths of 300 nm and varying widths of 100–400 nm. Axons of adult mouse sympathetic and sensory ganglia displayed contact guidance on all patterns (Figure 3C).[35] In our study, we have demonstrated that the likelihood that a neuron would align along nano-sized structures depends on the height of the ridges. We cultured primary leech neurons on substrates with ridges of heights from 150 nm and down to 10 nm (Figure 3D).[11] The majority of neuronal processes that approached ridges of 75 nm and higher were affected by the ridges and changed their original growth direction. However, when the topographic cues were smaller, the effect on growth was more selective, exhibiting a linear correlation between ridge height and the probability of alignment. On top of that, neurite orientation was shown to be determined not only by structural dimensions, but also by the approaching angle of the neurite. The incoming angle between the neuronal process and the topographical feature affects the interaction between the neuron and the topographical cue, particularly for ridges lower than 50 nm.[11] The incoming angles modified the "effective surface" for anchoring and influenced whether the neurite turns to follow the cue, or to cross the step to preserve its original direction.

3.1.2. Distribution of Topographical Features

Distance between anisotropic topographical cues has also been shown to be a factor in neurite guidance. The effects of distance on neuron directionality vary within the submicron to micron range, and are dependent on the ratio between height and width of topographical structures.[71] For 300 nm deep grooves and varying widths of 100–400 nm, patterns with 100 nm widths were less efficient in guiding axon orientation compared to larger-width patterns.[35] Lower grooves, with 200 nm depths, were shown to reduce PC12 neurite alignment from 90% to 75% when increasing the width of the plateaus and grooves from 500 to 750 nm.[41,103] Similarly, nano-gratings between 500 and 1500 nm were demonstrated to control the alignment of neurites as a function of the lateral ridge sizes.[71] In following studies, a computational model was developed to investigate the interactions of growth cones with such geometries to assess the average ridge width needed to achieve a given neurite alignment.[104–106] It should be specified that since grooves were investigated in these cases, larger widths of grooves mean smaller width of ridges and vice versa. Interestingly, the efficiency of guidance appeared to be related to the diameter of the axons; axons with 1 μm diameters or more were affected less than those with smaller diameters, probably due to mechanical properties and tensile forces that increase with diameter. Nevertheless, a study using parallel 350 nm high ridges showed that neurite orientation was not dependent on the spacing of the lines.[102] On the micro-scale, the effect of distance between topographical features on neuron alignment was shown to increase as the width of the space between cues decreased. PC12 cells on microgrooves (2–3 μm deep) exhibited statistically more significant parallel and aligned neurite growth on 5 μm grooves compared to larger grooves of 10 μm.[23] In addition, when PC12 cells were grown in micro-channels (11 μm height) with a distance of 20–60 μm range, the magnitude of impact on alignment of neurite growth depended on microchannel width, with the strongest orientation occurring in thinner grooves.[107] The pattern of neurite growth in response to grooved patterns does not seem to be uniform. Some studies show that neurites prefer to elongate in grooves, whereas other studies show neurite elongation atop ridges. For instance, neurites of PC12 cells cultured on patterned PLGA films showed a preference for growth in the microgrooves rather than on top of the elevated ridges.[23] In contrast, neurites of mouse sympathetic and sensory ganglia neurons grown on patterned poly(methyl methacrylate) (PMMA) silicon chips, preferred to grow on ridge edges and elevations in the patterns rather than in grooves.[35] These differences seem to depend on the width of lines and the distances between them. Although the specific dimensions at which neurons align according to anisotropic structures may vary between cell types, these studies suggest that topographical cues can be tailored to control neuronal alignment and organization.

3.1.3. Guidance on 3D Platforms

As with the patterned planar surfaces discussed above, 3D patterned structures, such as aligned fibers, hydrogels, nanowires and carbon nanotubes (CNTs), present an anisotropic topography for neuronal cells as well, and have been used for directing axonal growth.[48,75,86,108–113] Aligned fibers mimic the topography and orientation of structures that naturally occur in the mature nervous system. Culturing dorsal root ganglion (DRG) atop aligned electrospun fibers with 400–600 nm diameters resulted in neurite alignment parallel to the direction of the fibers.[31] Similarly, neural stem cells cultured on aligned PLLA fibrous scaffolds exhibited parallel neurite outgrowth,[47] and aligned nanofibers, consisting of PCL and gelatin, directed the growth of Schwann cells which oriented along the direction of the fibers in a longitudinal fashion.[114] In two following studies by Xie et al., DRG neurites extended along the long axis of oriented PCL nanofibers, which were shown to promote DRG adhesion and enhancement of neurite guidance and extension as compared with randomly oriented fibers.[26,115] Several parameters were taken into account, among them were fiber density and surface coating. Recently, our group developed

a method to remotely orient fibers by applying external magnetic fields to collagen hydrogels mixed with magnetic nanoparticles.[113] During the gelation period, the magnetic particles aggregated into magnetic particle strings, leading to the alignment of the collagen fibers. Ultimately, neurons were shown to form elongated morphology, relying on the particle strings and fibers as supportive cues for growth. In a following study, mechanical force was induced on the collagen gels by a controlled uniaxial strain, thus orienting the gel fibers and allowing neurites alignment.[112] Other effectors in these 3D structures which influence the alignment of the neurites are the diameter and size of fibers.[77,116] There is an optimal size range for the filament diameter for neurite guidance, in which filaments that are very large or very small relative to the size of the growth cone do not induce parallel alignment.[117] Effects on DRG neurites were most prominent on filaments with diameters in the range of cellular size and below (5 and 30 μm) where highly directional and robust neuronal outgrowth was achieved.

3.2. Effects on Processes

During development and growth, neurons outgrow neuronal processes—an axon and dendrites—from the cell soma, each with a unique morphological structure. In addition to neurite guidance abilities, surface topography has been reported to have a critical influence on the development of neurites, including neuritogenesis, neurite elongation and branching. These parameters are of great biological importance since they are directly related to neuronal polarization (i.e., providing dendrite-axon directionality to neurons), and thus, to the proper formation of neural networks. There have been a number of studies that focused on the influences of surface nanotopography on the onset of neuritogenesis or the rate of neurite elongation. Development of longer neurites on nanotopographies was mainly observed adjunctively in research efforts initially designed to show directional guidance effects of the substrates. For instance, Patel et al. showed that aligned PLLA nanofibers decorated with bioactive proteins could not only guide neurites, but also synergistically promote neurite outgrowth with certain types of proteins coated on the fibers.[75] Similar results have been observed in studies using cyclic olefin copolymer (COC) nanogratings,[71] electrospun PCL nanofibers,[26] carbon nanotubes,[110] silicon nanopillar arrays,[49] and gold nanoparticle-decorated polymeric nanofibers.[46] All of these examples clearly showed that surface topography, regardless of material, could guide the direction of neurite outgrowth as well as promote neurite outgrowth.

3.2.1. Promoted Neuronal Growth and Regeneration

As a general rule, anisotropic topographical features, which direct and orient neuronal processes (as mentioned above), enhance the elongation of neurites. Many studies have demonstrated that aligned neurons, on linear topographic structures or oriented fibers, show an increase in neurite length.[12,26,46,47,49,102] A representative example at the 2D level are micro-channels (polymide walls, 11 μm height, 20–60 μm width on glass substrate) which were shown to impact several properties of neurite growth.[107] Neurites emerging from cells grown in micro-channels were significantly longer than neurites emerging from control cells. In this study, neurites of cells grown in all micro-channels were longer than controls. However, no statistical difference in neurite length was observed for cells grown in micro-channels of different widths. Additionally, cell growth in the micro-channels significantly reduced the total number of neurites emerging per soma. The magnitude of the reduction in neurites depended on microchannel width. Similar results were shown for cultured neurons atop line-patterned substrates.[12] While the total neurite length atop the patterned substrates was significantly increased compared to flat substrates, the number of branching points and the number of originating neurites from the soma decreased (**Figure 4**A). Exceptions were reported by Miller et al. and by Yao et al. who showed that DRG neurites and PC12 cell neurites, respectively, cultured on smooth films had significantly higher elongation rates compared with neurites on microgrooved substrates.[23,93]

The effect of isotropic topography on neuron morphology has been widely studied as well. Isotropic topographical cues, such as evenly or randomly distributed pits, posts or pillars, demonstrate a significant effect on the typical elaboration and complexity of the dendritic tree. Scaffolds embedded with gold nanoparticles promote neurite regeneration and outgrowth as reflected by longer neurites and fewer branching points which lead to a more mature neuronal architecture.[46] Nanoparticle-coated substrates were also found to affect and promote the elongation of neurites of neuroblastoma SH-SY5Y cells. Alon et al. demonstrated a significant increase in number of neurites emerging from the soma on silver-nanoparticles substrates (AgNPs) compared to glass.[118] However, the effect is sensitive to the structure, as cells on nano-pillars and nano-pores developed fewer and shorter neurites.[119]

3.2.2. Neurite Outgrowth and Fate

Neuritogenesis and neurite outgrowth are biologically very sophisticated and multifaceted processes, and thus they cannot be fully understood simply by comparing the lengths or numbers of neurites. The in vitro development (i.e. that observed on cell-adhesive coverslips) of neurons has been studied extensively in the field of neural cell biology. The in vitro developmental pathway of primary hippocampal neurons was particularly well-defined by Dotti et al.,[120] who described it as follows: (i) stage 1: somas of neurons adhere to a coverslip and lamellipodia (F-actin based projections) form around the somas; (ii) stage 2: multiple indistinguishable neurites develop from the somas and start searching around the substrate; (iii) stage 3: one of the neurites (major neurite) starts to grow much faster than the others and the neurons become polarized; (iv) stage 4: the neurites except the major neurite grow and mature as well; (v) stage 5: finally, the neurons mature and exhibit functionality. Micholt et al. have demonstrated this atop pillars, showing preferred neuritogenesis towards the topography substrates (Figure 4B).[84] This developmental pathway is regarded as a global standard in many neural cell biology studies, however, it

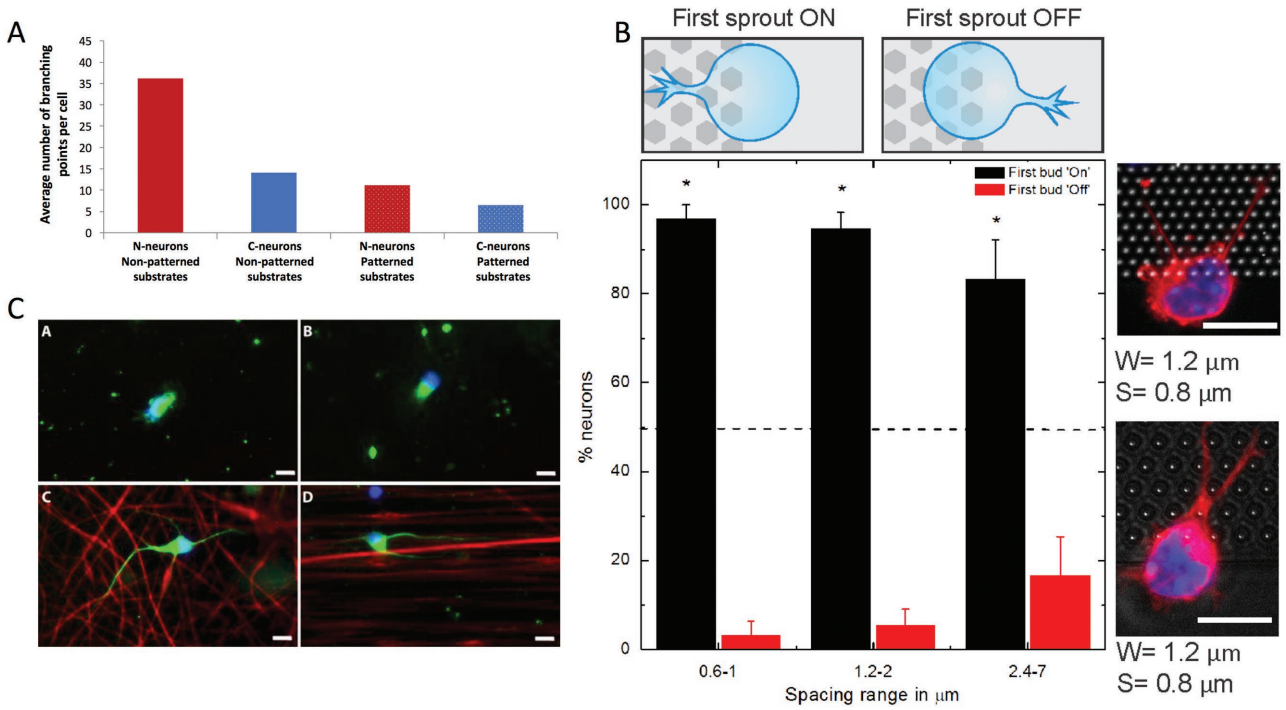

Figure 4. A) Average number of branching points on flat and patterned substrates. 'N', non-contact neurons; 'C', contact neurons. Reproduced with permission.[12] Copyright 2012, Springer. B) Analysis of the first sprout positioned towards (ON) or away (OFF) from the pillars. Blue, nuclei (Hoechst); Green, Golgi apparatus (GPP130); Red, microtubules (tuj-1); Grey, substrate; Scale bars 10 μm. Reproduced with permission.[84] Copyright 2013, PLOS. C) Motor neurons grown on glass (A), PLLA solvent-cast film (B), random fibers (C), and aligned fibers (D). Green, neurofilament; Red (C, D), sulforhodamine 101-positive fibers; Blue, DAPI; Scale bar 10 μm. Reproduced with permission.[8]

is uncertain that the development of neurons in vivo occurs in the same fashion.

In this respect, we and others have investigated neurite development on various surface topographies in terms of the above developmental stages. By culturing primary spinal motor neurons on PLLA electrospun nanofibers, Gertz et al. showed that aligned nanofibers not only elongated neurite lengths but also accelerated the polarization of neurons (i.e., a larger population of neurons in stage 3) (Figure 4C).[8] We examined the development of rat hippocampal neurons by using anodized aluminum oxide (AAO) substrates or silica nanobeads packed on a 2D surface. We found that such developmental acceleration broadly occurs on many types of nanotopographies, and also that there exists a threshold 'pitch' (a periodic distance between the top features of the surface topography) in eliciting the developmental acceleration from neurons cultured on top; the developmental acceleration occurred on the topographies that had a pitch larger than 200 nm (the first threshold),[88] and became more remarkable with increasing pitch size up to 1000 nm (the second threshold), above which the acceleration effect leveled off.[89] By conducting biochemical inhibition studies, we found that F-actin dynamics (formation/deformation of F-actins and actin-myosin contractility) play an indispensable role in recognizing different surface nanotopographies and eliciting intracellular changes accordingly for neurons.

More recently, we found that the same type of neurons adopted a completely new developmental pathway, rather than the conventional but accelerated pathway, on densely-packed vertically-grown silicon nanowires.[85] In contrast to the results on the other substrates, neurons on the nanowires sprouted a major neurite first right after plating, and this neurite elongated exclusively before other minor neurites developed. Despite this diversion from the conventional descriptions, during their development, neurons on the nanowires matured successfully and exhibited normal network functions at later stages. This may indicate that there is an alternative developmental pathway in primary hippocampal neurons which can be triggered by an extreme nanotopography like vertical nanowires. We also suspected that the newly found developmental pathway was reminiscent of what occurs in vivo, but the in vivo relevance of the new pathway still remains to be proven, because its biological mechanism is yet uncertain.

4. Intracellular Mechanisms Following Interactions with Topography

Most of the studies discussed above provided a quantitative morphological analysis of neuronal growth under the influence of micro- and nano- topographies, however, the effect of topography is not limited to morphological alterations alone. There is increasing evidence that indicates the ability of topography to trigger cellular responses and pathways.[41,74,90,121–123] This alone holds a great potential in the design of biomaterials for many indications, including drug delivery, regenerative medicine and more. In this section, we discuss modifications in

expression of proteins and genes following contact with topography and their role in these interactions.

4.1. Molecular Signaling Effects Following Neuronal Interactions with Topography

4.1.1. Cytoskeleton Remodeling and Adhesion

The major players in shaping the cells are the dynamic actin and microtubule cytoskeleton which are reorganized through signaling pathways that are linked to guidance cue receptors.[124] The earliest studies in neurons to deduce the signal transduction pathways which lead to cytoskeleton reorganization after contact with topography were conducted in 1997 by Rajnicek and McCaig (**Figure 5**A). They used inhibitors to show signal transduction pathways that are involved in alignment of hippocampal neurites on substrate topography.[74] In addition, calcium channels and protein kinase C were also involved in the orientation of these neurites. Since then researchers have been trying to elucidate more pathways that are involved in the interactions between neurons and topographical substrates.

One of the pathways that involve mechanical linkage between the cells and the substrate is focal adhesion (FA). These sites mediate the adhesion between integrin and the actin cytoskeleton and are influenced by the physical forces present in their extracellular environment.[13,125–127] In the context of topography, previous studies have shown alterations in FAs during neuronal growth atop nano-scale structures.[70,71,73,128] These alterations are less common on microscale structures due to the size of the FAs which is on the nano-scale range.[100] A major cytoskeletal protein associate with FAs, vinculin, was reported to be increased in C6 glioma-astrocytoma rat cell line cultured on nano-dot substrates, resulting in induced FA plaques.[128] As the alignment of neurites atop distinct topographies is controlled by mechanical forces, FAs are likely to affect this directionality, as described by Tonazzini et al. (Figure 5B).[70] Jang et al. suggested a crosstalk between two filopodia populations

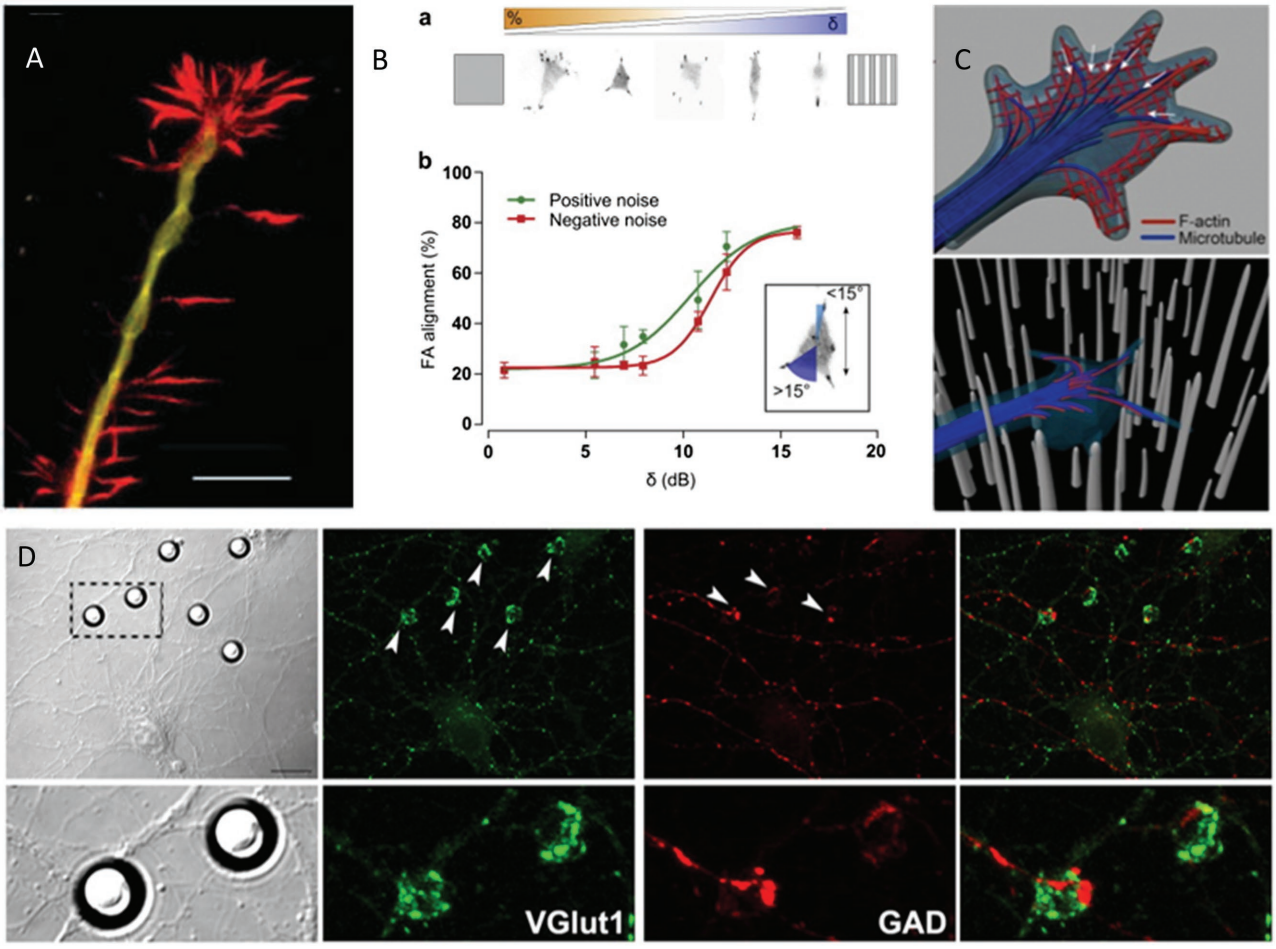

Figure 5. A) A confocal image of hippocampal neurite and growth cones. Red, filamentous actin; Green, α-tubulin. Scale bar 10 µm. Reproduced with permission.[63] Copyright 1997, The Company of Biologists. B) Impact of reduced substrate directionality on focal adhesion assembly and spatial distribution. a) EGFP-Paxillin-rich adhesions on noisy NGs. b) FA alignment as a function of substrate directionality δ, on positive (green line) and negative (red line) noise. Reproduced with permission.[70] Copyright 2013, Elsevier C) Microtubules and F-actin structures at the tips of the neurons on flat and *vg*-SiNW surfaces. Reproduced with permission.[85] Copyright 2015, American Chemical Society. D) PDL-coated beads induce the formation of adherent synaptic vesicle complexes on axons. Green, VGlut1; GAD, red; Scale bar 20 µm. Reproduced with permission.[130] Copyright 2009, Society for Neuroscience.

playing a role in sensing nanotopography for guiding neuronal growth.[102] This crosstalk lead to stabilization of the growth cone, and thus to steady neurite extension. Ubiquitin ligase E3a (UBE3A), which is thought to be associated with adhesion and cytoskeletal pathways, was found to play a role in neurite contact guidance on nanostructured substrates in deficient hippocampal neurons in which this gene was silenced.[122] These neurons were less aligned with the nanostructures, possibly suggesting an impaired activation of the FA pathway and reduction in cytoskeletal contractility. A different study by Brunetti et al. emphasized that by changing the physical properties of the surface nanostructures, they could control neuronal cell adhesion and growth.[73] The group showed that lack of organized focal adhesion points in SH-SY5Y cells growing atop nanorough substrates, leads to a loss of neuron polarity and activity. Moreover, the morphology of the Golgi apparatus was found to be abnormal, indicating an induced cell death by necrosis.

Neuronal polarity (i.e. the formation of axons and dendrites) is affected by topography as early as the first instant of initial contact establishment with the surface.[84] An indication of the initial neurite formation area can be predicted by *N*-cadherin and Golgi-centrosome complexes, which are co-localized at these sites. Micholt et al. showed enrichment of these complexes at micron-scale pillar contacts rather than on flat surfaces, following the positioning of an *N*-cadherin crescent.[84] In addition, tyrosine phosphorylation positions were observed together with F-actin aggregation and FAs accumulation (visualized by paxillin expression) at the pillar contacts. In our previous work using vertical nanowires, we suggested that changes in dynamic formation/deformation of F-actin structures can lead to different developmental pathways of neurons (Figure 5C).[85] Together, these results suggest neuronal polarization alterations induced by specific topographies, which were also shown to be preferred over chemical ligands.[68]

4.1.2. Artificial Synapse Formation

Another interesting aspect is the formation of synapses, termed synaptogenesis, which typically occurs between neighboring cells, but was also reported to form between artificial substrates and neuronal cells. Back in 1986, neurons cultured on coated beads developed presynaptic element even in the absence of a postsynaptic element.[129] These elements contained characteristics of mature pre-synapses such as synaptic vesicle antigens. Years after, this phenomenon of synapse assembly was investigated by Lucido et al. on hippocampal neurons using microbeads. They visualized functional presynaptic boutons assembled between the beads and the tip of the neurites by co-expression of the presynaptic markers VGlut1 and GAD (Figure 5D).[130] In two different studies by the same group, the formation of pre-synapses between sub-micrometer silica beads and hippocampal neurons was analyzed. These artificial synapses were visualized by cryo-electron microscopy and showed, as before, molecular features which exist at pre-synapses, such as presynaptic vesicles and microtubular structures.[131,132] In the same fashion, carbon nanotube islands induced the formation of synapses (based on synapsin staining) and the regulation of neuronal interconnections following mechanical attachment of neurites to the islands.[133] Interestingly, it has been reported that the expression of the gap-junction protein Cx43 was modulated by nano-topography.[128] Since gap-junction proteins are the major components of electrical synapse channels, this result indicates a role in cell-cell interactions as well. In our previous study, we showed that nano-topography triggers a modification in growth strategy similar to neuron-neuron interactions emphasizing the effect on neural interactions with artificial elements.[12] Collectively, these results raise many questions concerning the relationship between topography, function and form which are not fully understood and deserve further investigation.

4.2. Neuronal Differentiation

The ability of topography to control cell differentiation, especially that of stem cells, has been described extensively and has a significant importance for various therapeutic approaches. In most cases, the topography increased the differentiation rate even more efficiently than chemical induction, and resulted in distinct gene expression and protein level changes. These effects are dependent on the geometry and dimensions of the topography.

4.2.1. Cell Fate Determination by Topography

In the case of neural stem cells, the differentiation leads to two lineage fates: neuronal cells and glial cell (astrocytes and oligodendrocytes). The ability to determine cell fate is essential for brain repair and neural regeneration and distinct topography can provide a suitable microenvironment to manipulate neuronal stem cells. For example, parallel gratings of different depths were studied for their ability to affect the differentiation rate of neural progenitors into neurons.[98] Their results implied that the differentiation into a neuronal or astrocyte lineage is dependent on topography depth. The use of parallel gratings of increasing depth could enhance differentiation into neurons, independent of biochemical cues from the culture medium. Xie et al. examined the differentiation of embryonic stem cells (ESs) to neural lineage using randomly and uniaxially aligned PCL 250 nm fibers.[83] While ESs were capable of differentiating into mature neural lineage cells including neurons, oligodendrocytes and astrocytes, the aligned nanofibers could discourage the differentiation into astrocytes. Similarly, different topographical patterns can induce a different cell lineage, astrocytes or neurons. Linear micro-pattern and circular micro-pattern substrates with two different feature sizes (2 or 10 μm in width and spacing and 4 μm in depth) were reported to significantly enhance the differentiation of adult human neural stem cells (ANSCs) to neurons while depressing differentiation to astrocytes compared to control.[134] In this study, smaller feature sizes upregulated the differentiation of ANSCs into neurons. In addition, by using an ERK signaling inhibitor (U0126), it was suggested that MAPK/ERK pathway is partially involved in topography-induced differentiation; this pathway was previously shown to be involved in the regulation of neuronal differentiation. In two following studies by Yim's

group, gratings of varying lateral dimensions and height were used, in order to find whether different geometries and sizes play a role in neural differentiation and fate.[135,136] The group used multi-architectural chip (MARC) platforms which enable the use of micro- and nano-topographies simultaneously. The chip consisted of anisotropic gratings (2 μm gratings, 250 nm gratings) and isotropic 1 μm pillars. They found that anisotropic patterns promoted neuronal differentiation while isotropic patterns promoted the glial differentiation of stem and progenitor cells, as indicated by expression of β-III-tubulin. However, topography alone was insufficient and additional biochemical cues were necessary to fully achieve the desired effect. Remarkably, topographical cues could influence differentiation and lineage specification within different combinations of biochemical cues. A different approach was described by Low et al., in which differentiation to glial cells was reduced by siRNA-functionalized nanofibrous scaffolds, in favor of enhancing the differentiation to the neuronal lineage.[82] They incorporated siRNA with electrospun fibers as molecular mediators of differentiation for lineage-specific induction and used the RE-1 silencing transcription factor (REST), which acts as a repressor that is downregulated in neurogenesis. Overall, the rate of differentiation of neural progenitor cells to glial cells was lowered and a significantly higher percentage of neuronal cells was generated on siREST fibers than on fiber controls. It should be mentioned that neurons were also reported to respond strongly to the topography of glial cells, an observation that may prove useful for tissue-engineering strategies for nerve repair.[41]

4.2.2. Enhanced Differentiation Rate by Distinct Topography Dimensions

As the topography geometry and dimensions dictate the direction and morphology of the neuronal dendritic tree, they can also influence the differentiation rate and even enhance it without the use of chemical cues.[134,137–139] The choice of dimensions is critical and depends on many factors such as the cell type and its soma diameter. Based on these parameters, the width and depth of micro-patterned PDMS surfaces were designed for culturing ANSCs.[140] In this study, most of the cultured cells were found between the grooves and their adhesion rates were similar between the various widths and the control flat PDMS surfaces. However, the mean differentiation rate of the cells increased with the increase in width of the micro-channels compared to control surfaces. The number of neurites per cell and the polarity of the differentiated neurons were also affected; more neurites were originating from the soma as the width increased. The cells grew in a confined environment that demonstrated that groove width could influence the development and differentiation of the neural stem cells. Smaller grooves meant more contact area with the cell, which resulted in a decrease in neurites number, reminiscent of the growth strategy following contact with nanostructures, as discussed above. The effect of the pattern width on the differentiation rate was also investigated by nano- and micro-grating substrates.[72,141] Several neuronal markers were significantly upregulated on the nanostructured substrates compared to un-patterned and micro-patterned substrates, i.e. microtubule-associated protein 2 (MAP2). Notably, nanograting with a width of 350 nm showed a significant induction of neuronal marker expression, i.e. the neuroectodermal markers NPY and SYT4, as well as an improved differentiation efficiency and better homogeneity, based on upregulation of neuronal differentiation (NeuroD1 and NeuroG1) and neural crest (ISL1) markers.[72] The expression of Tuj1 (an immature neuronal marker) and Synaptophysin (**Figure 6**A) was also detected on the nanograting structures together with several other genes: SOX2, neurofilament light peptide (NFL) and tyrosine hydroxylase.[141] By using microarray technology, neuronal genes regulated by nanotopography were detected, i.e. brain-derived neurotrophic factor, synaptotagmin I and β-III-tubulin, among other genes related to ECM, adhesion molecule signaling and cell cycle, while genes related to glial differentiation were downregulated. These data provided evidence that the induction of neuronal differentiation was associated with alteration of ECM signaling or cytoskeleton arrangement.

4.2.3. 3D Platforms for Neuronal Differentiation

On the 3D level, both micro- and nano-scale fibers were investigated to show their ability to enhance neuronal differentiation.[47,137,142,143] Yang and co-authors grew C17.2 NSCs atop aligned PLLA fibers with 300 nm and 1.5 μm diameters.[47] The rate of differentiation was found to be higher for the nanofibers (80%) than for the microfibers (40%) and was independent of fiber alignment. In addition, the morphology of these cells was evaluated by immunostaining for neurofilaments, demonstrating that the aligned nanofibers highly supported the NSCs culture and improved neurite outgrowth. In a different 3D model, fibers ranging approximately between 280–1450 nm diameters were used to culture rat NSCs.[144] Here, the larger fibers promoted differentiation of neuronal cells due to the size of the fibers which limited the cell attachment and growth to a single fiber, whereas on 280 nm fibers, the cells could spread along the nanofiber matrix randomly, resulting in differentiation to the glial lineage (Figure 6B). However, Mahairaki et al., who used aligned and random 250 nm and 1 μm PCL fibers to investigate their effect on neural precursors (NPs), reported that the fiber orientation had a profound effect on the cell differentiation to the neuronal lineage, irrespective of diameter.[137] These conflicting results emphasize the difficulty of this field of research, since various materials and dimensions exert different effects on neuronal cells that also depend on the cell type. On the nano-scale, there is also sensitivity that can produce different effects on differentiation. When human-derived neural precursors were grown on aligned and random 400 and 800 nm tussah silk fibrion (TSF) scaffolds, differentiation was promoted on the aligned fibers and to a greater extent on the 400 nm diameter.[145] In a different study, three PCL fiber diameters were tested: 260, 480 and 930 nm together with their orientation.[146] ANSCs which were grown atop the 480 nm fibers, provided the strongest effect, based on Tuj1 and Nestin (marker for undifferentiated cells) staining. In correlation to the orientation, the alignment affected more than fibrous topography alone (Figure 6C). Interestingly, the topography was also found to drive the activation of canonical Wnt signaling pathway even

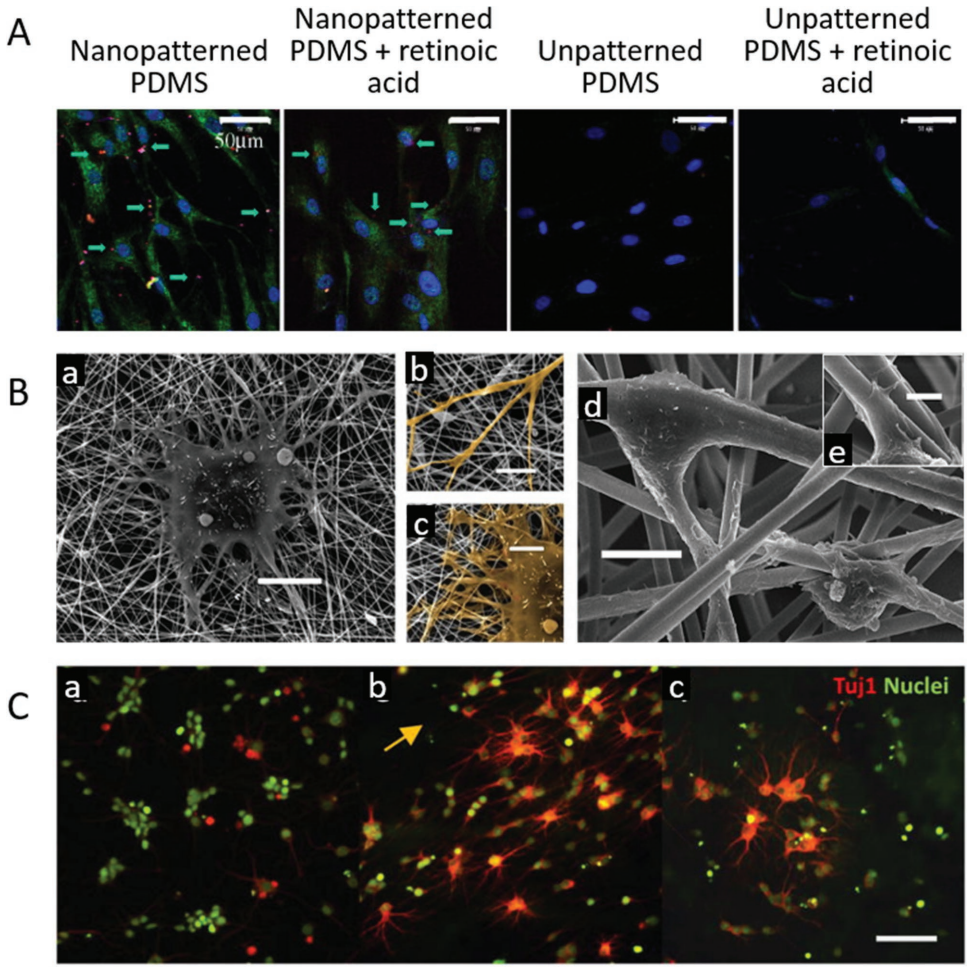

Figure 6. A) Immunofluorescence staining of synaptophysin (red) and MAP2 (green) of hMSCs cultured on patterned and unpatterned PDMS. Scale bars 50 μm. Reproduced with permission.[141] Copyright 2007, Elsevier. B) SEM images of rat NSCs cultured on 283 nm (a–c) and 1452 nm (d–e) fiber meshes. Scale bars 10 μm (a, d), 5 μm (b, c), 2 μm (e). Reproduced with permission.[144] Copyright 2009, Elsevier. C) Representative fluorescent images of ANSCs on planar surfaces (a), aligned 480 nm fiber (b) and random 480 nm fiber substrates. Scale bar 50 μm. Reproduced with permission.[146] Copyright 2010, Elsevier.

without soluble cues such as retinoic acid. This pathway has been shown to correlate with increased neurogenesis in ANSCs and the authors suggested that the dynamics of intracellular beta-catenin was influenced by structural rearrangements in ANSC morphology in response to the nanotopography.

Our group has shown the ability of nanoparticles to promote the differentiation of neuronal-like cells. The 10 nm gold nanoparticles that were embedded atop electrospun fibers have shown to improve cell adhesion and growth of differentiated PC12, even without the use of collagen coating which is considered essential for adherence and differentiation of these cells.[46] Similarly, in our previous work, the nerve growth factor (NGF), a differentiation inducer, was conjugated to free iron oxide nanoparticles and showed promotion of differentiation and outgrowth of the same cell type, as was described by the expression of several differentiation genetic markers.[147] PC12 growing in contact with nanostructure gratings made of biocompatible polymers were also used to study neuronal differentiation and topographical guidance.[50] By selective activation of specific molecular differentiation pathways, both contact guidance and the underlying establishment of cellular adhesions with the substrate could be differently modulated. For example, stimulation of PC12 cells with NGF or Forskolin led to a different number of initial adhesions with the substrate and to significant variation in the efficiency of neurite alignment to the nanogratings. Another parameter to be considered is the concentration of the chemical inducer. Different concentrations of NGF were used to differentiate PC12 atop surfaces with ridge widths ranging from 70 to 1900 nm.[148] The topographic feature size modulated the initiation of neurites from the cells when they were cultured with sub-optimal concentrations of NGF (25 and 5 ng/mL). Ridge widths ≤400 nm augmented neuritogenesis and ridge widths ≥850 nm pitch suppressed neuritogenesis. Moreover, ridges of 70 and 250 nm were shown to reduce the threshold for inductions of neuritogenesis. However, the alignment response of the neurites to the topography was independent of NGF concentration. A potential explanation for this observation is that NGF treatment leads to upregulation of integrin molecules in PC12 cells.[149,150] Thus, neurite adhesion may be controlled by

the nanostructures in the presence of low concentrations of growth factors.

In a review by McNamara et al., a mechanism by which topography affects cell differentiation was suggested.[151] According to this mechanism, the influence of the topography on cell adhesion is the key idea. These effects of topography are due to alterations in the surface area available for protein adsorption, restricting ECM deposition and therefore the size of the initial cell adhesions that can form. Furthermore, FAs, which involve integrin binding to ECM components, are related to the FA kinase and ERK pathways.[151] Both pathways were reported to affect cell differentiation. Moreover, ERK signaling is also required for the differentiation of PC12.[152] Together, these data seem to suggest that mechanotransduction most likely accounts for most of the physical changes in the cell.[153] Mechanotransduction of extracellular biophysical signals to the cell seems to account for the regulation of differentiation by topography which may be sensed via integrins and transmitted through FA signaling and the actin-cytoskeleton to the nucleus, ultimately leading to differential gene expression and differentiation into specific lineages.[135] Interestingly, from these studies we see a leading line which indicates that topography of 250–400 nm width, whether fiber or grating, was more efficient in affecting the differentiation rate. Even more remarkable is that aligned nanofibers enhanced the differentiation more than randomly organized fibers, similar to the nanograting described above, which raises the question of whether the linear geometry has a key role.

4.3. Topography for Improved Interfacing for Activity Monitoring

The basic mechanism of action of neurons, the action potential, which enables the cells to transmit information and communicate with each other, has an important role in the design of neural-based devices. A large body of research is concentrated on finding ways to investigate neuronal circuity by intracellular and extracellular recordings of neural networks. For instance, multielectrode arrays (MEA) are widely used for understanding neural network formation by measuring neuron activities over an extended period of time.[154–157] A variety of materials are being used to fabricate the electrodes, from planar gold, titanium and platinum to silicon[158] and graphene.[159–164] Since these types of MEAs have no topography and are designed and fabricated as flat substrates, their interactions with neurons are not included in the review. However, in order to improve MEA-neurons interface and to control cell migration and distribution atop the MEAs, the use of topography was suggested. One proposed approach was the use of topography to trap neurons in neuron-cages (**Figure 7**A),[165–167] however, the fabrication procedure is complicated and plating neurons inside the cages requires precision and is difficult to consistently achieve. A modification of this approach was studied by Xie and coauthors who used vertical nanopillars as a noninvasive neuron pinning to prevent cell migration during activity measurements (Figure 7B).[39] These nanopillars were of 1 μm height and 150 nm diameter and were fabricated on top of a customized MEA substrate. The nanopillars anchored the neurons and served as focal adhesion points for cell attachment, thus reducing cell body mobility without effecting neuronal growth. In the same line, gold microelectrodes (≈1.5 μm height) were developed for in-cell recording without mechanically damaging the cell's plasma membrane (Figure 7C).[168,169] The microspines that protrude from a flat substrate were engulfed by the cells through the activation of phagocytotic-like mechanisms. The engulfment was mediated by a peptide that improved the physical interface between the cell's plasma membrane and the substratum. The micro-structures were "swallowed" by the cell, allowing a tight adhesion between the plasma membrane and the head and stalk of the gold spine, thus enabling the generation of larger field potentials by action potentials of cultured neurons. Similar to the nanopillars, the tight warp with the vertical geometry led to a reduction of the membrane-electrode gap distance and higher seal resistance that is crucial for enhanced signal detection. These methods increase neuron-substrate adherence and electrical coupling and can eventually improve bi-directional coupling between cells and electronic devices.

Several other features have been used to improve the conductivity of neural networks for better circuitry. For instance, carbon nanotubes are widely used in nerve tissue engineering research due to their flexibility, electrical conductivity and mechanical strength. Their interactions with neuronal cells and their applications in neuroregeneration and repair have been reviewed recently,[170–173] thus we will only discuss it here briefly. Ballerini's group had chemically manipulated CNTs by adding solubilizing groups to their surface, which helped improving

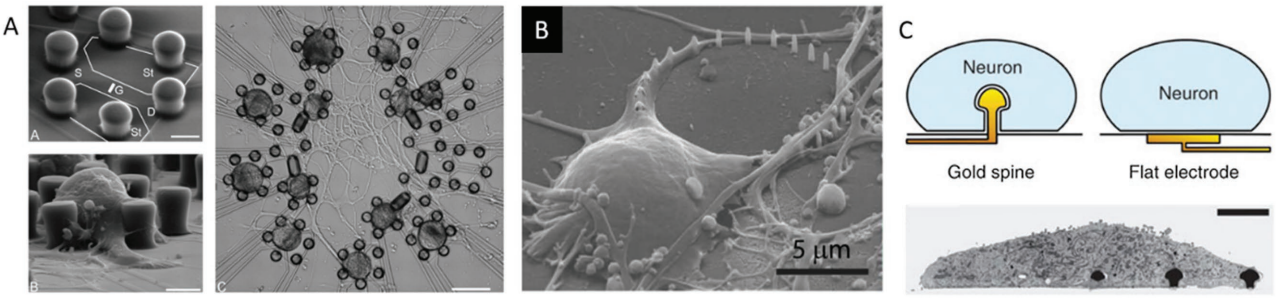

Figure 7. A) Electron micrographs of two-way contact with picket fence made of polyimide without (A) and with cells (B, C). Reproduced with permission.[166] Copyright 2001, National Academy of Sciences. B) A SEM image of a neuron with one of its neurites preferentially growing along the ring-shaped nanopillar arrays. Reproduced with permission.[39] Copyright 2010, American Chemical Society. C) Schematic representations (upper panel) and electron micrograph (lower panel) of neurons engulfing a gold-spine electrode. Reproduced with permission.[169] Copyright 2010, Nature Publishing Group.

their biocompatibility as well as nerve signaling.[174] They have shown that CNTs are able to favor synaptogenesis, thus affecting the neuronal communication. In a different study, the group has shown that 3D artificial scaffolds from multiwalled carbon nanotubes can guide the formation of neural webs in vitro, thus holds great potential for the development of future in vivo interfaces.[175] Another feature is nanowires that were also shown to closely interact with neurons and direct axonal growth. Dissociated sensory neurons were cultured on epitaxial gallium phosphide (GaP) nanowires grown vertically from a gallium phosphide surface.[87] The nanowires (2.5 μm long, 50 nm wide) supported cell adhesion and axonal outgrowth, and cell survival was better on nanowire substrates than on planar control substrates. The cells interacted closely with the nanostructures and were penetrated by hundreds of wires. This demonstrates the potential of incorporating nanowires within electronic devices to form strongly coupled interfaces with cell membranes and to measure signals from neurons.[176]

An emerging method, the use of conductive materials, has been used widely in recent years as scaffolds, for supporting neuronal growth and activity. Such materials include hydrogels and polymers that electrically regulate cellular activities.[177–182] Among these materials we can find polypyrrole (PPy),[183] poly(3,4-ethylenedioxythiophene) (PEDOT),[178,179,184,185] polyaniline (PANI)[177,186] and graphene oxide (GO).[187] The ability to electrically stimulate these materials have shown to affect, for example, the differentiation of NSCs while supporting cell attachment and proliferation.[177] The use of conductive polymers holds great potential in the regenerative medicine field. In an in vivo experiment, PEDOT filaments were shown to integrate directly within the surrounding of a living neuronal tissue in a way which may be possible to bypass the glial scar in order to reconnect to healthy neurons.[179] The use of such materials and others, e.g. silicon-metal wires,[5] will be invaluable for the design of new neural 3D interfaces for in vivo study.

5. Summary and Outlook

Many environmental cues have been shown to affect neuronal growth and guidance, including chemical cues, mechanical cues, growth factors and others. Here, we focused on physical topographical features of substrates that are used for manipulating neuronal fate and growth. As technology advances and fabrication abilities improve, synthetic topographies become better at mimicking native interactions that guide neurons throughout their development. Although neuronal interactions with synthetic substrates have been extensively studied, new facets of the underlying mechanisms remain to be elucidated. This review describes studies of substrates and 3D platforms decorated with a range of topographies, from micro-scale features down to topographical elements at the nanoscale, that have demonstrated effective interactions with neuronal cells. The smallest-scale features that have been reported here are in the range of 10 nm and their effects, together with the effects of all the features discussed in this review, are summarized in Table 1.

In the current progress report we have reviewed different aspects of effects of substrate topography on neurons. These effects depend on the geometry and dimensions of the topographical features. Topography has been shown to have a significant impact on neuronal growth, affecting morphology, including process formation, level of polarity and neurite directionality. Importantly, topography affects also functional mechanisms, from synapse formation to gene regulation. It has been shown that one of the major effectors in the interactions between the growing neurite and the substrate is the mechanical tension that is mediated by topography through cell adhesion, affecting intracellular elements. Neuronal differentiation was also found to be affected by topographical elements. In most cases, the topographical features increased the differentiation rate, even more efficiently than chemical induction. In the case of neural stem cells, their differentiation leads to two lineage fates: neuronal cells and glial cell (astrocytes and oligodendrocytes). The ability to determine cell fate is essential for brain repair and neural regeneration and distinct topography can provide a suitable microenvironment to manipulate neuronal stem cells.

Researchers in the field continuously strive to meet the challenge of integrating artificial elements with neuronal tissue. Considering the varying effects of different substrates on different neurons and matching them to specific needs may lead to the emergence of varying biomedical applications. In recent years applications based on topographic features for therapeutics or for profound brain-machine interface (BMI) have been developed, for instance, a micropatterning that allowed the study of mechanisms of myelin formation.[188–191] Here, new applications for both peripheral nerve regeneration using scaffolds,[189,190] and brain and spinal cord injury,[2,170] have been described.

To summarize, this progress report highlights the interplay between morphology and function of neuronal systems and the important roles played by topography. The research in this field is ongoing, and is expected to create a better, deeper understanding of neurogenesis and neuroregeneration mechanisms, ultimately enabling the generation of much-needed clinical solutions for patients suffering from neuronal injuries.

Acknowledgements

M.M. and K.B. contributed equally to this work. The authors thank Noa Alon for creating the abstract figure. O.S. thanks the Israel Science Foundation for partial support (#1053/15). I.S.C. thanks the financial support from the Basic Science Research Program through the National Research Foundation of Korea (NRF) funded by the Ministry of Science, ICT & Future Planning (MSIP) (2012R1A3A2026403).

Conflict of Interest

The authors declare no conflict of interest.

Keywords

contact guidance, nanofabrication, neuronal injury and regeneration, neuronal interfaces, topography

Received: March 1, 2017
Revised: May 7, 2017
Published online:

[1] P. A. Merolla, J. V. Arthur, R. Alvarez-Icaza, A. S. Cassidy, J. Sawada, F. Akopyan, B. L. Jackson, N. Imam, C. Guo, Y. Nakamura, B. Brezzo, I. Vo, S. K. Esser, R. Appuswamy, B. Taba, A. Amir, M. D. Flickner, W. P. Risk, R. Manohar, D. S. Modha, *Science* **2014**, *345*, 668.
[2] S. Shahdoost, S. Frost, G. Van Acker, S. DeJong, C. Dunham, S. Barbay, R. Nudo, P. Mohseni, Proc. 36th Annu. Int. IEEE, *Eng. Med. Biol. Soc.*, Chicago, USA, August **2014**, *2014*, 486.
[3] M. Jorfi, J. L. Skousen, C. Weder, J. R. Capadona, *J. Neural Eng.* **2015**, *12*, 011001.
[4] I. R. Minev, P. Musienko, A. Hirsch, Q. Barraud, N. Wenger, E. M. Moraud, J. Gandar, M. Capogrosso, T. Milekovic, L. Asboth, R. F. Torres, N. Vachicouras, Q. Liu, N. Pavlova, S. Duis, A. Larmagnac, J. Voros, S. Micera, Z. Suo, G. Courtine, S. P. Lacour, *Science* **2015**, *347*, 159.
[5] C. Xie, J. Liu, T. M. Fu, X. Dai, W. Zhou, C. M. Lieber, *Nat. Mater.* **2015**, *14*, 1286.
[6] T. Limongi, L. Tirinato, F. Pagliari, A. Giugni, M. Allione, G. Perozziello, P. Candeloro, E. Di Fabrizio, *Nano-Micro Lett.* **2016**, *9*, 1.
[7] A. M. Craig, G. Banker, *Ann. Rev. Neurosci.* **1994**, *17*, 267.
[8] C. C. Gertz, M. K. Leach, L. K. Birrell, D. C. Martin, E. L. Feldman, J. M. Corey, *Dev. Neurobiol.* **2010**, *70*, 589.
[9] I. B. Levitan, L. K. Kaczmarek, *The Neuron: Cell and Molecular Biology*, Oxford University Press, USA **2015**.
[10] M. Tessier-Lavigne, C. S. Goodman, *Science* **1996**, *274*, 1123.
[11] K. Baranes, N. Chejanovsky, N. Alon, A. Sharoni, O. Shefi, *Biotechnol. Bioeng.* **2012**, *109*, 1791.
[12] K. Baranes, D. Kollmar, N. Chejanovsky, A. Sharoni, O. Shefi, *J. Mol. Histol.* **2012**, *43*, 437.
[13] A. B. Huber, A. L. Kolodkin, D. D. Ginty, J. F. Cloutier, *Ann. Rev. Neurosci.* **2003**, *26*, 509.
[14] E. A. Vitriol, J. Q. Zheng, *Neuron* **2012**, *73*, 1068.
[15] E. J. Huang, L. F. Reichardt, *Ann. Rev. Neurosci.* **2001**, *24*, 677.
[16] M. G. Lykissas, A. K. Batistatou, K. A. Charalabopoulos, A. E. Beris, *Curr. Neurovasc. Res.* **2007**, *4*, 143.
[17] R. Levi-Montalcini, *Science* **1987**, *237*, 1154.
[18] C. E. Adler, R. D. Fetter, C. I. Bargmann, *Nat. Neurosci.* **2006**, *9*, 511.
[19] J. R. de la Torre, V. H. Höpker, G.-l. Ming, M.-m. Poo, M. Tessier-Lavigne, A. Hemmati-Brivanlou, C. E. Holt, *Neuron* **1997**, *19*, 1211.
[20] T. F. Sloan, M. A. Qasaimeh, D. Juncker, P. T. Yam, F. Charron, *PLoS Biol.* **2015**, *13*, e1002119.
[21] K. Brose, K. S. Bland, K. H. Wang, D. Arnott, W. Henzel, C. S. Goodman, M. Tessier-Lavigne, T. Kidd, *Cell* **1999**, *96*, 795.
[22] J. Dodd, T. M. Jessell, *Science* **1988**, *242*, 692.
[23] L. Yao, S. Wang, W. Cui, R. Sherlock, C. O'Connell, G. Damodaran, A. Gorman, A. Windebank, A. Pandit, *Acta Biomater.* **2009**, *5*, 580.
[24] P. K. Mattila, P. Lappalainen, *Nat. Rev. Mol. Cell. Biol.* **2008**, *9*, 446.
[25] G. Gallo, P. Letourneau, *Curr. Biol.* **2002**, *12*, R560.
[26] J. Xie, M. R. MacEwan, X. Li, S. E. Sakiyama-Elbert, Y. Xia, *ACS Nano* **2009**, *3*, 1151.
[27] J. Dzwonek, G. M. Wilczynski, *Front. Cell. Neurosci.* **2015**, *9*, 175.
[28] M. S. Deiner, T. E. Kennedy, A. Fazeli, T. Serafini, M. Tessier-Lavigne, D. W. Sretavan, *Neuron* **1997**, *19*, 575.
[29] D. M. Suter, P. Forscher, *J. Neurobiol.* **2000**, *44*, 97.
[30] J. P. Myers, M. Santiago-Medina, T. M. Gomez, *Dev. Neurobiol.* **2011**, *71*, 901.
[31] Y. T. Kim, V. K. Haftel, S. Kumar, R. V. Bellamkonda, *Biomaterials* **2008**, *29*, 3117.
[32] X. Gu, F. Ding, Y. Yang, J. Liu, *Prog. Neurobiol.* **2011**, *93*, 204.
[33] A. Subramanian, U. M. Krishnan, S. Sethuraman, *J. Biomed. Sci.* **2009**, *16*, 108.
[34] R. Deumens, A. Bozkurt, M. F. Meek, M. A. Marcus, E. A. Joosten, J. Weis, G. A. Brook, *Prog. Neurobiol.* **2010**, *92*, 245.
[35] F. Johansson, P. Carlberg, N. Danielsen, L. Montelius, M. Kanje, *Biomaterials* **2006**, *27*, 1251.
[36] F. Patolsky, B. P. Timko, G. Yu, Y. Fang, A. B. Greytak, G. Zheng, C. M. Lieber, *Science* **2006**, *313*, 1100.
[37] Y. Cui, Q. Wei, H. Park, C. M. Lieber, *Science* **2001**, *293*, 1289.
[38] C. Xie, Z. Lin, L. Hanson, Y. Cui, B. Cui, *Nat. Nanotechnol.* **2012**, *7*, 185.
[39] C. Xie, L. Hanson, W. Xie, Z. Lin, B. Cui, Y. Cui, *Nano Lett.* **2010**, *10*, 4020.
[40] M. E. Spira, A. Hai, *Nat. Nanotechnol.* **2013**, *8*, 83.
[41] D. Hoffman-Kim, J. A. Mitchel, R. V. Bellamkonda, *Ann. Rev. Biomed. Eng.* **2010**, *12*, 203.
[42] C. J. Bettinger, R. Langer, J. T. Borenstein, *Angew. Chem. Int. Ed.* **2009**, *48*, 5406.
[43] D. H. Kim, P. P. Provenzano, C. L. Smith, A. Levchenko, *J. Cell Biol.* **2012**, *197*, 351.
[44] M. Nikkhah, F. Edalat, S. Manoucheri, A. Khademhosseini, *Biomaterials* **2012**, *33*, 5230.
[45] Y. Li, K. A. Kilian, *Adv. Healthcare Mater.* **2015**, *4*, 2780.
[46] K. Baranes, M. Shevach, O. Shefi, T. Dvir, *Nano Lett.* **2016**, *16*, 2916.
[47] F. Yang, R. Murugan, S. Wang, S. Ramakrishna, *Biomaterials* **2005**, *26*, 2603.
[48] E. Schnell, K. Klinkhammer, S. Balzer, G. Brook, D. Klee, P. Dalton, J. Mey, *Biomaterials* **2007**, *28*, 3012.
[49] M. Park, E. Oh, J. Seo, M. H. Kim, H. Cho, J. Y. Choi, H. Lee, I. S. Choi, *Small* **2016**, *12*, 1148.
[50] A. Ferrari, P. Faraci, M. Cecchini, F. Beltram, *Biomaterials* **2010**, *31*, 2565.
[51] D. Y. Fozdar, J. Y. Lee, C. E. Schmidt, S. Chen, *Biofabrication* **2010**, *2*, 035005.
[52] R. G. Flemming, C. J. Murphy, G. A. Abrams, S. L. Goodman, P. F. Nealey, *Biomaterials* **1999**, *20*, 573.
[53] D. E. Discher, P. Janmey, Y. L. Wang, *Science* **2005**, *310*, 1139.
[54] J. H. Bell, J. W. Haycock, *Tissue Eng. Part B* **2012**, *18*, 116.
[55] L. A. Flanagan, Y. E. Ju, B. Marg, M. Osterfield, P. A. Janmey, *Neuroreport* **2002**, *13*, 2411.
[56] P. C. Georges, P. A. Janmey, *J. Appl. Physiol.* **2005**, *98*, 1547.
[57] P. C. Georges, W. J. Miller, D. F. Meaney, E. S. Sawyer, P. A. Janmey, *Biophy. J.* **2006**, *90*, 3012.
[58] S. Khan, G. Newaz, *J. Biomed. Mater. Res. Part A* **2010**, *93*, 1209.
[59] T. Elsdale, J. Bard, *J. Cell Biol.* **1972**, *54*, 626.
[60] P. Clark, P. Connolly, A. S. Curtis, J. A. Dow, C. D. Wilkinson, *Development* **1990**, *108*, 635.
[61] C. Oakley, D. M. Brunette, *J. Cell Sci.* **1993**, *106*, 343.
[62] P. Clark, P. Connolly, A. S. Curtis, J. A. Dow, C. D. Wilkinson, *Development* **1987**, *99*, 439.
[63] A. Rajnicek, S. Britland, C. McCaig, *J. Cell Sci.* **1997**, *110*, 2905.
[64] M. E. Hatten, *Trends Neurosci.* **1990**, *13*, 179.
[65] A. Webb, P. Clark, J. Skepper, A. Compston, A. Wood, *J. Cell Sci.* **1995**, *108*, 2747.
[66] B. Zhu, Q. Zhang, Q. Lu, Y. Xu, J. Yin, J. Hu, Z. Wang, *Biomaterials* **2004**, *25*, 4215.
[67] I. Tonazzini, E. Jacchetti, S. Meucci, F. Beltram, M. Cecchini, *Adv. Healthcare Mater.* **2015**, *4*, 1849.
[68] N. Gomez, S. Chen, C. E. Schmidt, *J. R. Soc. Interface* **2007**, *4*, 223.
[69] I. Nagata, A. Kawana, N. Nakatsuji, *Development* **1993**, *117*, 401.
[70] I. Tonazzini, S. Meucci, P. Faraci, F. Beltram, M. Cecchini, *Biomaterials* **2013**, *34*, 6027.
[71] A. Ferrari, M. Cecchini, A. Dhawan, S. Micera, I. Tonazzini, R. Stabile, D. Pisignano, F. Beltram, *Nano Lett.* **2011**, *11*, 505.
[72] F. Pan, M. Zhang, G. Wu, Y. Lai, B. Greber, H. R. Scholer, L. Chi, *Biomaterials* **2013**, *34*, 8131.

[73] V. Brunetti, G. Maiorano, L. Rizzello, B. Sorce, S. Sabella, R. Cingolani, P. P. Pompa, *Proc. Natl. Acad. Sci. USA* **2010**, *107*, 6264.
[74] A. Rajnicek, C. McCaig, *J. Cell Sci.* **1997**, *110*, 2915.
[75] S. Patel, K. Kurpinski, R. Quigley, H. Gao, B. S. Hsiao, M. M. Poo, S. Li, *Nano Lett.* **2007**, *7*, 2122.
[76] J. M. Corey, D. Y. Lin, K. B. Mycek, Q. Chen, S. Samuel, E. L. Feldman, D. C. Martin, *J. Biomed. Mater. Res. Part A* **2007**, *83*, 636.
[77] H. B. Wang, M. E. Mullins, J. M. Cregg, C. W. McCarthy, R. J. Gilbert, *Acta Biomater.* **2010**, *6*, 2970.
[78] W. J. Li, C. T. Laurencin, E. J. Caterson, R. S. Tuan, F. K. Ko, *J. Biomed. Mater. Res.* **2002**, *60*, 613.
[79] Z. Ma, M. Kotaki, R. Inai, S. Ramakrishna, *Tissue Eng.* **2005**, *11*, 101.
[80] Z. Q. Feng, T. Wang, B. Zhao, J. Li, L. Jin, *Adv. Mater.* **2015**, *27*, 6462.
[81] N. Li, Q. Zhang, S. Gao, Q. Song, R. Huang, L. Wang, L. Liu, J. Dai, M. Tang, G. Cheng, *Sci. Rep.* **2013**, *3*, 1604.
[82] W. C. Low, P. O. Rujitanaroj, D. K. Lee, P. B. Messersmith, L. W. Stanton, E. Goh, S. Y. Chew, *Biomaterials* **2013**, *34*, 3581.
[83] J. Xie, S. M. Willerth, X. Li, M. R. Macewan, A. Rader, S. E. Sakiyama-Elbert, Y. Xia, *Biomaterials* **2009**, *30*, 354.
[84] L. Micholt, A. Gartner, D. Prodanov, D. Braeken, C. G. Dotti, C. Bartic, *PLoS One* **2013**, *8*, e66170.
[85] K. Kang, Y. S. Park, M. Park, M. J. Jang, S. M. Kim, J. Lee, J. Y. Choi, H. Jung da, Y. T. Chang, M. H. Yoon, J. S. Lee, Y. Nam, I. S. Choi, *Nano Lett.* **2016**, *16*, 675.
[86] C. Prinz, W. Hallstrom, T. Martensson, L. Samuelson, L. Montelius, M. Kanje, *Nanotechnology* **2008**, *19*, 345101.
[87] W. Hallstrom, T. Martensson, C. Prinz, P. Gustavsson, L. Montelius, L. Samuelson, M. Kanje, *Nano Lett.* **2007**, *7*, 2960.
[88] K. Kang, S. E. Choi, H. S. Jang, W. K. Cho, Y. Nam, I. S. Choi, J. S. Lee, *Angew. Chem. Int. Ed.* **2012**, *51*, 2855.
[89] K. Kang, S. Y. Yoon, S. E. Choi, M. H. Kim, M. Park, Y. Nam, J. S. Lee, I. S. Choi, *Angew. Chem. Int. Ed.* **2014**, *53*, 6075.
[90] J. Y. Lim, H. J. Donahue, *Tissue Eng.* **2007**, *13*, 1879.
[91] S. B. Jun, M. R. Hynd, N. Dowell-Mesfin, K. L. Smith, J. N. Turner, W. Shain, S. J. Kim, *J. Neurosci. Methods* **2007**, *160*, 317.
[92] M. Kwiat, R. Elnathan, A. Pevzner, A. Peretz, B. Barak, H. Peretz, T. Ducobni, D. Stein, L. Mittelman, U. Ashery, F. Patolsky, *ACS Appl. Mater. Interfaces* **2012**, *4*, 3542.
[93] C. Miller, S. Jeftinija, S. Mallapragada, *Tissue Eng.* **2002**, *8*, 367.
[94] H. Sorribas, C. Padeste, L. Tiefenauer, *Biomaterials* **2002**, *23*, 893.
[95] R. V. Bellamkonda, *Biomaterials* **2006**, *27*, 3515.
[96] J. W. Lee, K. S. Lee, N. Cho, B. K. Ju, K. B. Lee, S. H. Lee, *Sens. Actuators, B* **2007**, *128*, 252.
[97] H. Hwang, G. Kang, J. H. Yeon, Y. Nam, J. K. Park, *Lab Chip* **2009**, *9*, 167.
[98] J. S. Chua, C. P. Chng, A. A. Moe, J. Y. Tann, E. L. Goh, K. H. Chiam, E. K. Yim, *Biomaterials* **2014**, *35*, 7750.
[99] N. Gomez, Y. Lu, S. Chen, C. E. Schmidt, *Biomaterials* **2007**, *28*, 271.
[100] M. Arnold, E. A. Cavalcanti-Adam, R. Glass, J. Blummel, W. Eck, M. Kantlehner, H. Kessler, J. P. Spatz, *ChemPhysChem* **2004**, *5*, 383.
[101] A. S. Curtis, M. Dalby, N. Gadegaard, *Nanomedicine* **2006**, *1*, 67.
[102] K. J. Jang, M. S. Kim, D. Feltrin, N. L. Jeon, K. Y. Suh, O. Pertz, *PLoS One* **2010**, *5*, e15966.
[103] M. Cecchini, A. Ferrari, F. Beltram, *J. Phys. Conf. Ser.*, Stockholm, Sweden, March **2008**, *100*, 012003.
[104] P. N. Sergi, I. Morana Roccasalvo, I. Tonazzini, M. Cecchini, S. Micera, *PLoS One* **2013**, *8*, e70304.
[105] I. M. Roccasalvo, P. N. Sergi, I. Tonazzini, M. Cecchini, S. Micera, *Proc. 37th Annu. Int. IEEE Eng. Med. Biol. Soc.,* Milan, Italy, August **2015**, *2015*, 7147.
[106] P. N. Sergi, A. Marino, G. Ciofani, *Integr. Biol.* **2015**, *7*, 1242.
[107] M. J. Mahoney, R. R. Chen, J. Tan, W. M. Saltzman, *Biomaterials* **2005**, *26*, 771.
[108] J. M. Corey, C. C. Gertz, B. S. Wang, L. K. Birrell, S. L. Johnson, D. C. Martin, E. L. Feldman, *Acta Biomater.* **2008**, *4*, 863.
[109] G. Dos Reis, F. Fenili, A. Gianfelice, G. Bongiorno, D. Marchesi, P. E. Scopelliti, A. Borgonovo, A. Podesta, M. Indrieri, E. Ranucci, P. Ferruti, C. Lenardi, P. Milani, *Macromol. Biosci.* **2010**, *10*, 842.
[110] M. J. Jang, S. Namgung, S. Hong, Y. Nam, *Nanotechnology* **2010**, *21*, 235102.
[111] J. M. Zuidema, M. M. Pap, D. B. Jaroch, F. A. Morrison, R. J. Gilbert, *Acta Biomater.* **2011**, *7*, 1634.
[112] M. Antman-Passig, S. Levy, C. Gartenberg, H. Schori, O. Shefi, *Tissue Eng.* **2017**, *23*, 403.
[113] M. Antman-Passig, O. Shefi, *Nano Lett.* **2016**, *16*, 2567.
[114] D. Gupta, J. Venugopal, M. P. Prabhakaran, V. R. Dev, S. Low, A. T. Choon, S. Ramakrishna, *Acta Biomater.* **2009**, *5*, 2560.
[115] J. Xie, W. Liu, M. R. MacEwan, P. C. Bridgman, Y. Xia, *ACS Nano* **2014**, *8*, 1878.
[116] S. Gnavi, B. E. Fornasari, C. Tonda-Turo, G. Ciardelli, M. Zanetti, S. Geuna, I. Perroteau, *Mater. Sci. Eng. C Mater. Biol. Appl.* **2015**, *48*, 620.
[117] X. Wen, P. A. Tresco, *J. Biomed. Mater. Res. A* **2006**, *76*, 626.
[118] N. Alon, Y. Miroshnikov, N. Perkas, I. Nissan, A. Gedanken, O. Shefi, *Int. J. Nanomedicine* **2014**, *9* Suppl 1, 23.
[119] F. Haq, V. Anandan, C. Keith, G. Zhang, *Int. J. Nanomedicine* **2007**, *2*, 107.
[120] C. G. Dotti, C. A. Sullivan, G. A. Banker, *J. Neurosci.* **1988**, *8*, 1454.
[121] R. Rauti, N. Lozano, V. Leon, D. Scaini, M. Musto, I. Rago, F. P. Ulloa Severino, A. Fabbro, L. Casalis, E. Vazquez, K. Kostarelos, M. Prato, L. Ballerini, *ACS Nano* **2016**, *10*, 4459.
[122] I. Tonazzini, S. Meucci, G. M. Van Woerden, Y. Elgersma, M. Cecchini, *Adv. Healthcare Mater.* **2016**, *5*, 850.
[123] R. Kriparamanan, P. Aswath, A. Zhou, L. Tang, K. T. Nguyen, *J. Nanosci. Nanotechnol.* **2006**, *6*, 1905.
[124] K. Kalil, E. W. Dent, *Curr. Opin. Neurobiol.* **2005**, *15*, 521.
[125] M. A. Wozniak, K. Modzelewska, L. Kwong, P. J. Keely, *Biochim. Biophys. Acta* **2004**, *1692*, 103.
[126] D. D. Schlaepfer, C. R. Hauck, D. J. Sieg, *Prog. Biophys. Mol. Biol.* **1999**, *71*, 435.
[127] M. A. Schwartz, M. H. Ginsberg, *Nat. Cell biol.* **2002**, *4*, E65.
[128] C. H. Lee, Y. W. Cheng, G. S. Huang, *Nanoscale Res. Lett.* **2014**, *9*, 250.
[129] R. W. Burry, *Neurochem. Pathol.* **1986**, *5*, 345.
[130] A. L. Lucido, F. Suarez Sanchez, P. Thostrup, A. V. Kwiatkowski, S. Leal-Ortiz, G. Gopalakrishnan, D. Liazoghli, W. Belkaid, R. B. Lennox, P. Grutter, C. C. Garner, D. R. Colman, *J. Neurosci.* **2009**, *29*, 12449.
[131] G. Gopalakrishnan, P. Thostrup, I. Rouiller, A. L. Lucido, W. Belkaid, D. R. Colman, R. B. Lennox, *ACS Chem. Neurosci.* **2010**, *1*, 86.
[132] G. Gopalakrishnan, P. T. Yam, C. Madwar, M. Bostina, I. Rouiller, D. R. Colman, R. B. Lennox, *ACS Chem. Neurosci.* **2011**, *2*, 700.
[133] S. Anava, A. Greenbaum, E. Ben Jacob, Y. Hanein, A. Ayali, *Biophys. J.* **2009**, *96*, 1661.
[134] L. Qi, N. Li, R. Huang, Q. Song, L. Wang, Q. Zhang, R. Su, T. Kong, M. Tang, G. Cheng, *PLoS One* **2013**, *8*, e59022.
[135] A. A. Moe, M. Suryana, G. Marcy, S. K. Lim, S. Ankam, J. Z. Goh, J. Jin, B. K. Teo, J. B. Law, H. Y. Low, E. L. Goh, M. P. Sheetz, E. K. Yim, *Small* **2012**, *8*, 3050.
[136] S. Ankam, M. Suryana, L. Y. Chan, A. A. Moe, B. K. Teo, J. B. Law, M. P. Sheetz, H. Y. Low, E. K. Yim, *Acta Biomater.* **2013**, *9*, 4535.
[137] V. Mahairaki, S. H. Lim, G. T. Christopherson, L. Xu, I. Nasonkin, C. Yu, H. Q. Mao, V. E. Koliatsos, *Tissue Eng. Part A* **2011**, *17*, 855.

[138] E. Migliorini, G. Grenci, J. Ban, A. Pozzato, M. Tormen, M. Lazzarino, V. Torre, M. E. Ruaro, *Biotechnol. Bioeng.* **2011**, *108*, 2736.
[139] L. Y. Chan, W. R. Birch, E. K. Yim, A. B. Choo, *Biomaterials* **2013**, *34*, 382.
[140] A. Beduer, C. Vieu, F. Arnauduc, J. C. Sol, I. Loubinoux, L. Vaysse, *Biomaterials* **2012**, *33*, 504.
[141] E. K. Yim, S. W. Pang, K. W. Leong, *Exp. Cell Res.* **2007**, *313*, 1820.
[142] X. Jiang, H. Q. Cao, L. Y. Shi, S. Y. Ng, L. W. Stanton, S. Y. Chew, *Acta Biomater.* **2012**, *8*, 1290.
[143] M. K. Horne, D. R. Nisbet, J. S. Forsythe, C. L. Parish, *Stem Cells Dev.* **2010**, *19*, 843.
[144] G. T. Christopherson, H. Song, H. Q. Mao, *Biomaterials* **2009**, *30*, 556.
[145] J. Wang, R. Ye, Y. Wei, H. Wang, X. Xu, F. Zhang, J. Qu, B. Zuo, H. Zhang, *J. Biomed. Mater. Res. Part A* **2012**, *100*, 632.
[146] S. H. Lim, X. Y. Liu, H. Song, K. J. Yarema, H. Q. Mao, *Biomaterials* **2010**, *31*, 9031.
[147] M. Marcus, H. Skaat, N. Alon, S. Margel, O. Shefi, *Nanoscale* **2015**, *7*, 1058.
[148] J. D. Foley, E. W. Grunwald, P. F. Nealey, C. J. Murphy, *Biomaterials* **2005**, *26*, 3639.
[149] Z. Zhang, G. Tarone, D. C. Turner, *J. Biol. Chem.* **1993**, *268*, 5557.
[150] K. Danker, N. Mechai, L. Lucka, W. Reutter, R. Horstkorte, *Biol. Chem.* **2001**, *382*, 969.
[151] L. E. McNamara, R. J. McMurray, M. J. Biggs, F. Kantawong, R. O. Oreffo, M. J. Dalby, *J. Tissue Eng.* **2010**, *2010*, 120623.
[152] L. J. Klesse, L. F. Parada, *Microsc. Res. Tech.* **1999**, *45*, 210.
[153] D. E. Koser, A. J. Thompson, S. K. Foster, A. Dwivedy, E. K. Pillai, G. K. Sheridan, H. Svoboda, M. Viana, L. D. Costa, J. Guck, C. E. Holt, K. Franze, *Nat. Neurosci.* **2016**, *19*, 1592.
[154] S. M. Potter, T. B. DeMarse, *J. Neurosci. Methods* **2001**, *110*, 17.
[155] R. Segev, M. Benveniste, E. Hulata, N. Cohen, A. Palevski, E. Kapon, Y. Shapira, E. Ben-Jacob, *Phys. Rev. Lett.* **2002**, *88*, 118102.
[156] D. A. Wagenaar, R. Madhavan, J. Pine, S. M. Potter, *J. Neurosci.* **2005**, *25*, 680.
[157] M. E. Obien, K. Deligkaris, T. Bullmann, D. J. Bakkum, U. Frey, *Front. Neurosci.* **2014**, *8*, 423.
[158] I. Schoen, P. Fromherz, *J.Neurophysiol.* **2008**, *100*, 346.
[159] D. Kireev, S. Seyock, J. Lewen, V. Maybeck, B. Wolfrum, A. Offenhausser, *Adv. Healthcare Mater.* **2017**, *6*, 1601433.
[160] W. L. Rutten, *Ann. Rev. Biomed. Eng.* **2002**, *4*, 407.
[161] C. D. James, A. J. Spence, N. M. Dowell-Mesfin, R. J. Hussain, K. L. Smith, H. G. Craighead, M. S. Isaacson, W. Shain, J. N. Turner, *IEEE Trans. Biomed. Eng.* **2004**, *51*, 1640.
[162] L. Berdondini, P. Massobrio, M. Chiappalone, M. Tedesco, K. Imfeld, A. Maccione, M. Gandolfo, M. Koudelka-Hep, S. Martinoia, *J. Neurosci. Methods* **2009**, *177*, 386.
[163] U. Frey, U. Egert, F. Heer, S. Hafizovic, A. Hierlemann, *Biosens. Bioelectron.* **2009**, *24*, 2191.
[164] J. H. Kim, G. Kang, Y. Nam, Y. K. Choi, *Nanotechnology* **2010**, *21*, 85303.
[165] M. P. Maher, J. Pine, J. Wright, Y. C. Tai, *J. Neurosci. Methods* **1999**, *87*, 45.
[166] G. Zeck, P. Fromherz, *Proc. Natl. Acad. Sci. USA* **2001**, *98*, 10457.
[167] J. Erickson, A. Tooker, Y. C. Tai, J. Pine, *J. Neurosci. Methods* **2008**, *175*, 1.
[168] A. Hai, A. Dormann, J. Shappir, S. Yitzchaik, C. Bartic, G. Borghs, J. P. Langedijk, M. E. Spira, *J. R. Soc., Interface* **2009**, *6*, 1153.
[169] A. Hai, J. Shappir, M. E. Spira, *Nat. Methods* **2010**, *7*, 200.
[170] A. Fabbro, M. Prato, L. Ballerini, *Adv. Drug Delivery Rev.* **2013**, *65*, 2034.
[171] A. Sucapane, G. Cellot, M. Prato, M. Giugliano, V. Parpura, L. Ballerini, *J. Nanoneurosci.* **2009**, *1*, 10.
[172] M. David-Pur, L. Bareket-Keren, G. Beit-Yaakov, D. Raz-Prag, Y. Hanein, *Biomed. Microdev.* **2014**, *16*, 43.
[173] D. Rand, Y. Hanein, in *Nanotechnology and Neuroscience: Nano-electronic, Photonic and Mechanical Neuronal Interfacing* (Eds: M. De Vittorio, L. Martiradonna, J. Assad), Springer, New York, USA **2014**, p. 1.
[174] S. Bosi, A. Fabbro, C. Cantarutti, M. Mihajlovic, L. Ballerini, M. Prato, *Carbon* **2016**, *97*, 87.
[175] S. Usmani, E. R. Aurand, M. Medelin, A. Fabbro, D. Scaini, J. Laishram, F. B. Rosselli, A. Ansuini, D. Zoccolan, M. Scarselli, M. De Crescenzi, S. Bosi, M. Prato, L. Ballerini, *Sci. Adv.* **2016**, *2*, e1600087.
[176] B. P. Timko, T. Cohen-Karni, Q. Qing, B. Tian, C. M. Lieber, *IEEE Trans. Nanotechnol.* **2010**, *9*, 269.
[177] B. Xu, T. Bai, A. Sinclair, W. Wang, Q. Wu, F. Gao, H. Jia, S. Jiang, W. Liu, *Mater. Today Chem.* **2016**, *1–2*, 15.
[178] S. Sekine, Y. Ido, T. Miyake, K. Nagamine, M. Nishizawa, *J. Am. Chem. Soc.* **2010**, *132*, 13174.
[179] S. M. Richardson-Burns, J. L. Hendricks, D. C. Martin, *J. Neural Eng.* **2007**, *4*, L6.
[180] T. Nyberg, A. Shimada, K. Torimitsu, *J.Neurosci. Methods* **2007**, *160*, 16.
[181] R. A. Green, S. Baek, L. A. Poole-Warren, P. J. Martens, *Sci. Technol.Adv. Mater.* **2010**, *11*, 014107.
[182] J. Goding, A. Gilmour, P. Martens, L. Poole-Warren, R. Green, *Adv. Healthcare Mater.* **2017**, *6*, 1601177.
[183] Z. Shi, H. Gao, J. Feng, B. Ding, X. Cao, S. Kuga, Y. Wang, L. Zhang, J. Cai, *Angew. Chem. Int. Ed.* **2014**, *53*, 5380.
[184] W. Guo, X. Zhang, X. Yu, S. Wang, J. Qiu, W. Tang, L. Li, H. Liu, Z. L. Wang, *ACS Nano* **2016**, *10*, 5086.
[185] D. N. Heo, S. J. Song, H. J. Kim, Y. J. Lee, W. K. Ko, S. J. Lee, D. Lee, S. J. Park, L. G. Zhang, J. Y. Kang, S. H. Do, S. H. Lee, I. K. Kwon, *Acta Biomater.* **2016**, *39*, 25.
[186] V. Guarino, M. A. Alvarez-Perez, A. Borriello, T. Napolitano, L. Ambrosio, *Adv. Healthcare Mater.* **2013**, *2*, 218.
[187] C. Gardin, A. Piattelli, B. Zavan, *Trends Biotechnol.* **2016**, *34*, 435.
[188] D. Liazoghli, A. D. Roth, P. Thostrup, D. R. Colman, *ACS Chem. Neurosci.* **2012**, *3*, 90.
[189] X. Gu, F. Ding, D. F. Williams, *Biomaterials* **2014**, *35*, 6143.
[190] J. Xie, M. R. MacEwan, W. Liu, N. Jesuraj, X. Li, D. Hunter, Y. Xia, *ACS Appl. Mater. Interfaces* **2014**, *6*, 9472.
[191] K. M. Oprych, R. L. Whitby, S. V. Mikhalovsky, P. Tomlins, J. Adu, *Adv. Healthcare Mater.* **2016**, *5*, 1253.

